Australian Government
Department of Defence
Defence Science and
Technology Organisation

Comparison of Engineering Correlations for Predicting Heat Transfer in Zero-pressure-gradient Compressible Boundary Layers with CFD and Experimental Data

K. Higgins

Air Vehicles Division

Defence Science and Technology Organisation

DSTO–TR–2159

ABSTRACT

The aim of this report is to investigate the details and performance of several engineering correlation methods used for predicting skin friction and heat transfer rates in high-speed flows. These are the van Driest, Eckert and Spalding & Chi correlations, which, in the form presented herein, can only be used for zero-pressure-gradient flows. This limits the scope of the report to flow past flat plates, and also wedges and cones with attached shock waves. The main result is a series of comparisons with experimental and CFD data of Stanton Numbers, heat transfer rates, skin friction coefficients and viscous length scales computed with the engineering correlations. Good agreement was observed among the laminar correlation, CFD and experimental data. Comparisons of turbulent correlation results with CFD and experimental data produced reasonable agreement in most cases, although the van Driest and Eckert correlations tended to over-estimate heat transfer rates on cold walls.

Published by

DSTO Defence Science and Technology Organisation
506 Lorimer St,
Fishermans Bend, Victoria 3207, Australia

Telephone: (03) 9626 7000
Facsimile: (03) 9626 7999

AR No. 014-237
August, 2008

APPROVED FOR PUBLIC RELEASE

Comparison of Engineering Correlations for Predicting Heat Transfer in Zero-pressure-gradient Compressible Boundary Layers with CFD and Experimental Data

Executive Summary

DSTO's participation in the HIFiRE hypersonic vehicle flight test program has renewed interest in aerodynamic heating in high-speed flows. Robust design of such vehicles requires knowledge of the rate of surface heating experienced during hypersonic flight. For vehicles of simple geometry, heating rates can be estimated very quickly using empirical methods. More detailed analysis requires the use of computational fluid dynamics (CFD). Although CFD offers some advantages, it is, by comparison with empirical methods, more difficult to implement and produces results less rapidly. For these reasons, it is likely that empirical methods (referred to herein as 'engineering correlations') will be used in some stages of the design of hypersonic vehicles in the HIFiRE Program.

The aim of the work reported here is to investigate the details and performance of several engineering correlation methods used for predicting skin friction and heat transfer rates in high-speed flows. The fundamental equations used to compute these quantities are provided, and a description of the van Driest, Eckert and Spalding & Chi engineering correlations then follows. These correlations, in the form presented herein, can only be used for zero-pressure-gradient flows. The scope of this report is therefore limited to flow past flat plates, and also wedges and cones with attached shock waves. The correlation methods for these geometries are implemented in a Fortran 90 code for a mixture of calorifically imperfect species and arbitrary reference conditions. Both laminar and turbulent compressible boundary layers are considered, but transition is not modelled.

The main result of this report is a series of comparisons of Stanton Numbers, heat transfer rates, skin friction coefficients and viscous length scales computed using the engineering correlations with experimental and CFD data. For high-enthalpy flat plate boundary layers with Mach Numbers in the range 4.4–6.7 and a wall temperature of 300 K, reasonable agreement between the laminar Eckert, laminar CFD and experimental Stanton Numbers was obtained. For the turbulent cases, the Spalding, van Driest and Eckert correlations tended to bracket the cluster of experimental measurements, while the turbulent CFD results fell somewhere between these lower and upper limits. It was also concluded that the van Driest and Eckert correlations tended to over-estimate heat transfer rates on cold walls, thereby somewhat compensating for the absence of a transition model. For a 5° semi-angle cone at Mach 7.9, the engineering correlations and CFD significantly under-predicted the experimental turbulent Stanton Numbers for a wall-to-stagnation temperature ratio of 0.35. For cooler-wall cases, the agreement between the experimental data and van Driest and Eckert correlations improved significantly. Heat transfer rates for a Mach 8 flat plate, 10° semi-angle wedge and cone at an altitude of 35 km were also computed. These cases were examined because they are representative of a Mach Number and altitude that might be encountered in the HIFiRE flight test program. It was found that the local heat transfer rates 1.0 m from the leading edge of the wedge and cone were larger than the Mach 8 flat plate result by factors of 3.5 and 3.0 respectively. Finally, heat transfer rates for Mach 5 and 6 flat plates immersed in vitiated air were computed for the proposed hypersonic wind tunnel at DSTO-Melbourne. Turbulent local heat transfer rates for the Mach 6 case were found to be 30% larger than those experienced by a Mach 8 flat plate at altitude.

Author

Dr Keith Higgins
Air Vehicles Division

Keith Higgins completed a Bachelor of Engineering with Honours (Mechanical) and a Bachelor of Science at The University of Melbourne in 1998. During his undergraduate studies, he was included on the Annual Dean's Honours Lists for Science twice, and for Engineering, four times. He was also awarded the A. G. M. Mitchell prize for outstanding academic results at the end of his final year of Mechanical Engineering.

Keith joined Corporate Value Associates in 1999 as a Management Consultant, and spent a year in their London office working on several projects for Lloyds Bank in their Business Banking and Credit Card divisions. In 2000 he commenced his Ph.D studies in the Department of Mechanical Engineering at the University of Melbourne. His doctoral research was in the field of vortex dynamics, and it produced a model of fluid turbulence using numerical solutions of the Navier-Stokes equations. His Ph.D thesis 'A numerical study of turbulent fine scales' was passed in 2004. The thesis was awarded the University's 2004 Dr John Patterson Prize and the 2005 M. H. de Fina Prize.

Keith has published three refereed journal papers in the field of vortex dynamics; one in *Journal of Fluid Mechanics* and two in *Physics of Fluids*. He was invited to give seminars on his Ph.D research at the Graduate Aeronautical Laboratories at California Institute of Technology in 2001, and at the Department of Applied Mathematics and Theoretical Physics at Cambridge University in 2002. He also gave a lecture at the 2001 IUTAM–NATO Symposium on Tubes, Sheets and Singularities in Fluid Dynamics.

Keith has always had a strong interest in teaching and learning, and was a well-known Tutor at the University of Melbourne in Mathematics and Mechanical Engineering. He was also the Resident Tutor in Mathematics at Trinity College at the University of Melbourne during 2001 and 2002. His other responsibilities there included acting as an academic and professional development mentor for a group of resident students, and also serving as the Secretary of the Senior Common Room.

After completing his Ph.D, Keith continued working at The University of Melbourne as a Tutor in Mathematics and Mechanical Engineering during 2005. At this time he became interested in a career in quantitative finance, and he completed an honours-level subject on financial derivative pricing in the Faculty of Economics and Commerce at the University of Melbourne. He finished at the top of his class and was awarded the 2005 Citigroup Prize for 333-618 Advanced Derivative Securities.

In March 2006, Keith started working as a contractor in the Aircraft Signature Management (ASM) group in Air Vehicles Division at DSTO Melbourne. He subsequently joined the ASM group in October 2006 to work on the HIFiRE program. However, he maintains a strong link to the University of Melbourne, and, from September 2008, he will be giving 18 lectures on the numerical solution of partial differential equations for the honours-level subject *Advanced Computational Mechanics* in the Department of Mechanical Engineering.

Contents

Appendices

Figures

Tables

1 Introduction

Objects immersed in high-speed fluid flows experience aerodynamic heating. This effect is caused by viscous dissipation and the conversion of kinetic energy into thermal energy in the boundary layers surrounding the object. Renewed interest in aerodynamic heating has been generated by DSTO's involvement in the HIFiRE program, which aims to fly research vehicles at hypersonic velocities (i.e. over five times the speed of sound).

The surface temperatures and heat transfer rates experienced by hypersonic vehicles are important inputs for their structural design and materials selection. Among the methods available for predicting aerodynamic heating, analytical and empirical techniques provide rough estimates and are quick and easy to use. On the other hand, computational fluid dynamics (CFD) methods are generally more difficult to implement and produce results more slowly.

It is anticipated that empirical techniques (hereafter referred to as 'engineering correlations') will play an important role in the early phase of HIFiRE vehicle design, and a solid understanding of the details and limitations of these methods is therefore required. This is achieved herein by comparing predictions from a range of well-known engineering correlations with CFD results and experimental data. These comparisons are made for zero-pressure-gradient boundary layer flows on flat plates, wedges and cones.

The report begins with a description of how the wall heat transfer rate can be computed in a boundary-layer flow. The methods of van Driest (1956), Spalding & Chi (1964) and Eckert (1955) are then outlined. These are engineering correlations for predicting laminar and turbulent local skin friction coefficients, viscous length scales and heat transfer rates in zero-pressure-gradient boundary layers. The author has implemented these methods in a Fortran 90 code called `zpg_qdot` for a mixture of calorifically imperfect species and arbitrary reference conditions. Both laminar and turbulent boundary layers are considered, but transition is not modelled. Therefore, results from `zpg_qdot` are either laminar or turbulent, and caution would be required when using these results near a point of boundary layer transition. (Readers of this report who are interested in transition are referred to Anderson 1989.) Since zero-pressure-gradient boundary layers occur on flat plates, wedges and cones, `zpg_qdot` can be used to compute local heat transfer rates in all three cases. Optional inputs also allow `zpg_qdot` to compute local radiation and wall heat transfer rates and wall temperatures. Instructions for running `zpg_qdot` are given, and sample input and output files are provided.

The main result of this report is a series of comparisons of the engineering correlations implemented in `zpg_qdot` with experimental and CFD data. These comparisons include high-enthalpy hypersonic flat plate boundary layers and various Mach 7.9 5° semi-angle cone boundary layers. Other comparisons with CFD data only are made for Mach 8 flat plates and 10° semi-angle wedges and cones at an altitude of 35 km. Total heat transfer rates are also considered at this altitude for flat plates with Mach Numbers in the range 5–10. These flat plate, wedge and cone cases were selected because they provide some useful comparisons of heat transfer rates in the range of Mach Numbers and an altitude that might be encountered in the HIFiRE flight test program. Finally, a comparison to CFD data for Mach 5 and Mach 6 vitiated air flat plate boundary layers is made. These cases are relevant to the design of a proposed hypersonic wind tunnel at DSTO-Melbourne.

The details of the CFD, obtained with a finite-volume structured mesh Navier–Stokes code based on the method of White & Morrison (1999), and outputs of `zpg_qdot` could be of interest to scientists in the HIFiRE program. For this reason, the details of the computational grids, numerical method inputs and `zpg_qdot` input and output files are documented in a series of Appendices.

2 Zero-pressure-gradient compressible boundary layers

In the following discussion, a zero-pressure-gradient compressible boundary layer develops on a surface with wall-normal coordinate y. The velocity component parallel to the surface is u, and the surface temperature is T_w. In all cases, the subscripts e and 0 indicate free-stream static and total quantities respectively.

2.1 Local skin friction coefficient

The local skin friction coefficient is defined as

$$c_f = \frac{\tau_w}{\frac{1}{2}\rho_e u_e^2}, \tag{1}$$

where τ_w is the surface shear stress at $y = 0$ and ρ_e and u_e are the free-stream static density and velocity. Here

$$\tau_w = \mu_w \left[\frac{\partial u}{\partial y}\right]_{y=0}, \tag{2}$$

where μ_w is the dynamic viscosity of the fluid at the wall.

Next, the friction velocity is defined as

$$u_\tau = \sqrt{\frac{\tau_w}{\rho_w}}, \tag{3}$$

where ρ_w is the density of the fluid at the wall. The friction velocity can be used to scale the wall-normal velocity profile in a turbulent boundary layer, where

$$u^+ = u/u_\tau \quad \text{versus} \quad y^+ = y u_\tau/\nu_w \tag{4}$$

is the 'inner-layer' scaling of the velocity profile. Here $\nu_w = \mu_w/\rho_w$ is the kinematic viscosity of the fluid at the wall.

2.2 Viscous length scale

A common problem in CFD is to determine the distance from the wall to the first grid point in order to keep $y^+ = O(1)$ there. If $y^+ = 1$ at the first grid point, then $y/(\nu_w/u_\tau) = 1$ from the second of (4). Therefore, if

$$\delta_\nu = \frac{\nu_w}{u_\tau} \tag{5}$$

is defined as the viscous length scale, then the dimensional distance from the wall to the first grid point should equal δ_ν. The viscous length scale may also be written in terms of the local skin friction coefficient by substitution of (1) and (2) into (5), with the result

$$\delta_\nu = \frac{\mu_w}{u_e}\left(\frac{2}{\rho_e \rho_w}\right)^{1/2} c_f^{-1/2}. \tag{6}$$

2.3 Local heat transfer rate

Anderson (1989, pp. 248–249) outlines the process for computing heat transfer to a surface in high-speed flow. Briefly, the local heat transfer rate is

$$\dot{q} = \rho_e u_e C_H (h_{aw} - h_w), \tag{7}$$

where C_H is the Stanton Number and h_{aw} and h_w are the adiabatic wall enthalpy and the wall enthalpy respectively. To take into account irreversible processes in the boundary layer flow, the adiabatic wall enthalpy may be expressed in terms of a recovery factor r as

$$h_{aw} = h_e + r(h_0 - h_e), \tag{8}$$

where h_e and h_0 are the free-stream static and total enthalpies respectively. At this point it is convenient to introduce the Prandtl Number

$$Pr = \frac{c_p \mu_e}{k}, \tag{9}$$

where c_p is the specific heat at constant pressure, μ_e is the free-stream dynamic viscosity and k is the thermal conductivity of the fluid. The recovery factor is typically written in terms of the Prandtl Number as

$$r = Pr^{1/2} \quad \text{for laminar flow, and} \tag{10a}$$

$$r = Pr^{1/3} \quad \text{for turbulent flow.} \tag{10b}$$

The Prandtl Number is usually an input into heat transfer calculations, and a typical assumption is $Pr = 0.71$ for air at standard conditions (Anderson, 1989, p. 242).

The Stanton Number can be eliminated from the expression for the local heat transfer rate (7) using a Reynolds analogy

$$\frac{2C_H}{c_f} = R_f, \tag{11}$$

where R_f is the Reynolds analogy factor. Hence (7) becomes

$$\dot{q} = \tfrac{1}{2} \rho_e u_e R_f c_f (h_{aw} - h_w), \tag{12}$$

thereby linking the local heat transfer rate to an expression for the local skin friction coefficient which can be determined empirically. For laminar flow, the Reynolds analogy factor is typically assumed to be $R_f = Pr^{-2/3}$ (see Anderson, 1989, p. 250). For turbulent flow, Bradshaw (1977) suggests a value of $R_f = 1.1$. Hopkins & Inouye (1971) recommends $R_f = 1.0$ for hypersonic turbulent boundary layers with significant wall cooling, and $R_f = 1.2$ for adiabatic wall conditions (see also Cary, 1970).

2.4 Compressibility transformations

Goyne *et al.* (2003) outlines compressibility transformation methods that can be used to compare compressible flow skin friction data, obtained from a range of experimental conditions, with a single incompressible skin friction expression. The compressibility transformation can be written in terms of the functions F_c and F_{Re_x} as

$$c_{f,i} = F_c c_f \quad \text{and} \tag{13a}$$

$$Re_{x,i} = F_{Re_x} Re_x, \tag{13b}$$

where

$$Re_x = \rho_e u_e x / \mu_e \tag{14}$$

is the Reynolds Number based on the distance x from the leading edge of the plate. The subscript i in (13a) and (13b) indicates an incompressible value of the associated variable.

To compute the local skin friction coefficient for a compressible boundary layer at x with Reynolds Number Re_x, the associated incompressible Reynolds Number $Re_{x,i}$ is first computed from (13b). The local skin friction coefficient is then computed from an empirical correlation. Two correlations typically used are (Anderson, 1989, pp. 286–287)

$$c_{f,i} = 0.6640 Re_{x,i}^{-0.5} \quad \text{for a laminar boundary layer, and} \tag{15a}$$

$$c_{f,i} = 0.0592 Re_{x,i}^{-0.2} \quad \text{for a turbulent boundary layer.} \tag{15b}$$

The compressible local skin friction coefficient c_f may then be obtained from (13a). Three compressibility transformations (i.e. specific choices of F_c and F_{Re_x}) are described in the following paragraphs.

2.4.1 van Driest (1956)

This correlation is valid for turbulent boundary layers only. Here

$$F_c = \frac{T_{aw}/T_e - 1}{(\sin^{-1}\kappa + \sin^{-1}\nu)^2} \quad \text{and} \tag{16a}$$

$$F_{Re_x} = \frac{\mu_e}{\mu_w}\frac{1}{F_c}, \tag{16b}$$

where

$$\kappa = \frac{T_{aw}/T_e + T_w/T_e - 2}{\left[(T_{aw}/T_e + T_w/T_e)^2 - 4T_w/T_e\right]^{1/2}} \quad \text{and} \tag{17a}$$

$$\nu = \frac{T_{aw}/T_e - T_w/T_e}{\left[(T_{aw}/T_e + T_w/T_e)^2 - 4T_w/T_e\right]^{1/2}}, \tag{17b}$$

where T_w and T_{aw} are the wall and adiabatic wall temperatures respectively (which can be computed from the wall and adiabatic wall enthalpies), and T_e is the free-stream static temperature.

2.4.2 Spalding & Chi (1964)

This correlation is valid for turbulent boundary layers only. Here

$$F_c = \frac{T_{aw}/T_e - 1}{(\sin^{-1}\kappa + \sin^{-1}\nu)^2} \quad \text{and} \tag{18a}$$

$$F_{Re_x} = \frac{(T_{aw}/T_e)^{0.772}(T_w/T_e)^{-1.474}}{F_c}, \tag{18b}$$

where κ and ν are given by (17a) and (17b).

2.4.3 Eckert (1955)

This method is valid for laminar and turbulent boundary layers. For the reference temperature method,

$$F_c = T^*/T_e \quad \text{and} \tag{19a}$$

$$F_{Re_x} = \frac{\mu_e T_e}{\mu^* T^*}, \tag{19b}$$

where the reference temperature is

$$T^* = 0.5T_w + 0.22T_{aw} + 0.28T_e. \tag{20}$$

The adiabatic wall temperature in (20) should be evaluated with a recovery factor based on a Prandtl Number $Pr^* = \mu^* c_p^*/k^*$ evaluated at the reference temperature, thereby requiring iteration to determine T^*. However, this is not implemented in the present code `zpg_qdot` because it cannot compute the thermal conductivity of an arbitrary mixture of species. However, this is not a significant problem because the recovery factor is only a weak function of the Prandtl Number, and the Prandtl Number varies only slightly with temperature.

For the reference enthalpy method, the reference enthalpy is

$$h^* = 0.5h_w + 0.22h_{aw} + 0.28h_e, \tag{21}$$

from which T^* and μ^* may be computed for use in (19a) and (19b).

2.5 Total heat transfer rate

The total heat transfer rate per unit plate width at distance x from the leading edge of a flat plate is

$$\dot{Q}(x) = \int_0^x \dot{q}(x')\mathrm{d}x'. \tag{22}$$

By substitution of (12)–(15b) into (22) and integrating, it is not difficult to show that

$$\dot{Q}(x) = \frac{0.664\rho_e^{0.5}u_e^{0.5}\mu_e^{0.5}}{F_c F_{Re_x}^{0.5}} R_f(h_{aw} - h_w)x^{0.5} \quad \text{for a laminar boundary layer, and} \tag{23a}$$

$$\dot{Q}(x) = \frac{0.037\rho_e^{0.8}u_e^{0.8}\mu_e^{0.2}}{F_c F_{Re_x}^{0.2}} R_f(h_{aw} - h_w)x^{0.8} \quad \text{for a turbulent boundary layer.} \tag{23b}$$

3 Implementation of engineering correlations

The engineering correlation methods outlined in sections 2.4.1–2.4.3 for zero-pressure-gradient boundary layers were implemented by the author in a Fortran 90 code called `zpg_qdot`. This code makes use of `cmpexp` written by Dr. Nigel Smith from Air Vehicles Division at DSTO. The code `cmpexp` uses the CHEMKIN subroutine library (Kee *et al.*, 1980) to treat mixtures of calorifically imperfect gases. Additional routines have been incorporated by Dr. Smith that allow the effect of isentropic and shock changes to be determined for these gases with either frozen or equilibrium chemical compositions. The VODE package (Brown *et al.*, 1989) for stiff ordinary differential equations is used to solve the equations associated with these processes.

3.1 Installing and compiling `zpg_qdot`

Readers of this report who would like a copy of the `zpg_qdot` source code can obtain this from the author in the form of a gzipped tar file called `zpg_qdot.tgz`. This contains the `zpg_qdot` source code and sample input and output files.

In their own home directory, the user should uncompress and unpack the gzipped tar file using the command `tar -xvzf zpg_qdot.tgz`. This makes a new directory `zpg_qdot` containing the subdirectories `bin`, `dat`, `docs`, `run` and `src`. The directory `run` contains a subdirectory `zpg_example` with sample input files and scripts. The directory `src` contains the source code in the file `zpg_qdot.f90`, and also all other source code files needed for `cmpexp`. Provided that the user has a `bin` directory in their home directory, the code may be compiled by typing `make`. The binaries can be copied into `zpg_qdot/bin` by typing `./.bincopy`.

3.2 Running `zpg_qdot` for flat plates

Figure 1 shows a flowchart of the inputs and outputs for the programs `cmpexp` and `zpg_qdot`. Table 1 lists the input files and scripts used to run the codes. Example inputs files for a Mach 8 flat plate can be found in `zpg_qdot/run/zpg_example/fltplt_M8`.

The codes may be run using these steps:

1. Edit the input file `interpin.d` which contains a list of elements and species used by the code. (This step will probably be unnecessary in most cases.)

2. Run the script `.setup` using the command `./.setup`. This will produce three new input files `interpout.d`, `reactdata.d` and `thermdat.d`.

3. Edit the `cmpexp` input file `1ns`. An example of this input file is shown in figure 2 for a Mach 8 flat plate at an altitude of 35 km. For flat plate cases, the only parameters that should be changed in `1ns` are the free-stream static pressure, Mach Number, static temperature and species mass fractions. These parameters are listed in `1ns` as `initial_pressure`, `initial_mach_number`, `default_initial_temperature`, and under `>SPC`.

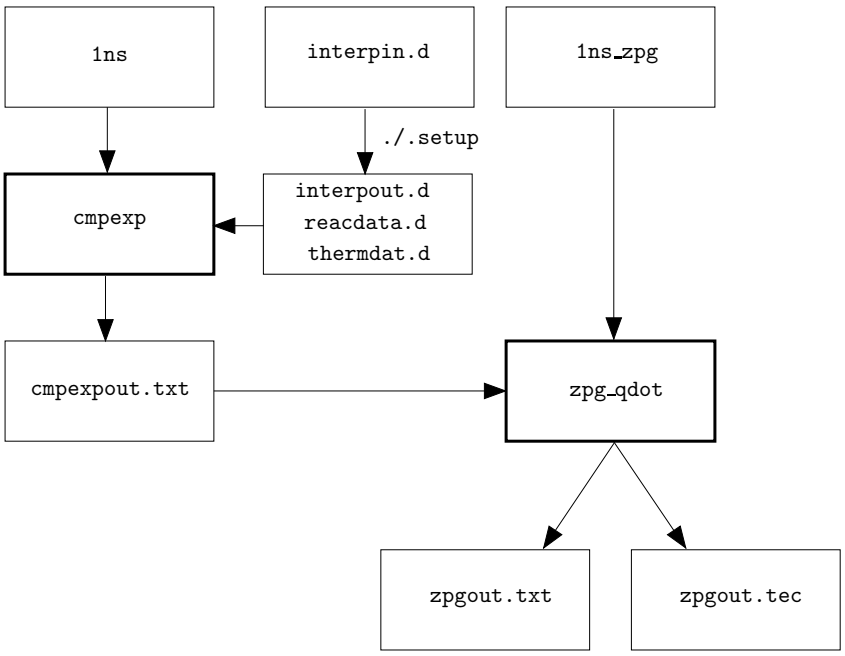

Figure 1: Input and output flowchart for `cmpexp` and `zpg_qdot`.

`interpin.d`	input file listing elements and species
`1ns`	input instructions file for `cmpexp`
`1ns_zpg`	input instructions file for `zpg_qdot`
`.setup`	script to set up chemical input data for `cmpexp`
`.run`	script to run `cmpexp` only
`.clear`	script to remove output files for `cmpexp` only
`.zpg_run`	script to run `cmpexp` and `zpg_qdot`
`.zpg_clear`	script to remove output files for `cmpexp` and `zpg_qdot`

Table 1: Input files for `cmpexp` and `zpg_qdot` and scripts used to run the codes.

```
>---

>TXT
        ***** Mach 8.00 flat plate inflow conditions *****
>END

>PRM
     &CMEX_PARAMETERS initial_pressure = 574.42,
                       initial_mach_number = 8.00,
                     default_initial_temperature = 236.47 /

     >SPC
         2
         N2  0.77
         O2  0.23
     >END

     >RUN
        2
        ISEN 1.0e0
        SHCK 1.300
     >END

     >RCT
        &REAC_PARAMETERS /
     >END

     >VOD
        &VODE_PARAMETERS /
     >END

>END

>---
```

Figure 2: Input file `1ns` for `cmpexp` for Mach 8 flat plate.

```
            &ZPG_QDOT_PARAMETERS T_wall = 300.0,
                    platelength = 1.0,
                                xpoints = 100,
                              shockcase = 0,
                           RefTempMethod = 1,
                                 prandtl = 0.72,
                Reynolds_analogy_factor = 1.1 /
```

Figure 3: Input file `1ns_zpg` for `zpg_qdot` for Mach 8 flat plate.

4. Edit the `zpg_qdot` input file `1ns_zpg`. An example of this input file is shown in figure 3. The first two parameters in `1ns_zpg` are `T_wall` and `platelength`. The parameter `xpoints` controls the number of evenly-spaced stream-wise coordinates on the plate in the Tecplot output data file. The integer parameter `shockcase` should be set to `0` for flat plates. The integer parameter `RefTempMethod` selects the type of reference temperature method that is used:

`1`	Eckert (1955)
`2`	White (1974)
`3`	Anderson (1989)

   The last two parameters in the file are `prandtl` and `Reynolds_analogy_factor`.

5. Run `zpg_qdot` using the script `./.zpg_run` by typing the command `./.zpg_run`. Two output files will be produced. First, a text file `zpgout.txt` containing a table of c_f, δ_ν and $\dot{q}$ evaluated at `platelength` from the leading edge of the plate for each correlation. An example of this output file for a Mach 8 flat plate at an altitude of 35 km is shown in figure 4. Note that there is a section in this example output file for radiation and wall heat transfer rates. When the optional inputs in the file `1ns_zpq` required for this calculation (discussed in section 3.4) are not supplied, a default `Case 0` is assumed in which all convective heat transfer is absorbed by the isothermal wall. In this case, `qdot` equals the wall heat transfer rate `qw_dot`. The second output is a Tecplot data file `zpgout.tec` containing c_f, δ_ν and $\dot{q}$ evaluated at `xpoints` evenly-spaced coordinates along the length of the plate for each correlation.

6. The output files may be removed by typing `./.zpg_clear`.

Dimensionless heat transfer results are often presented in the literature by plotting the Stanton Number against the logarithm of the Reynolds Number Re_x based on the distance from the leading edge of the plate. It was thought that this would be a useful feature to include in `zpg_qdot`, and it can be activated by adding three optional inputs to the file `1ns_zpg`:

Input	Description
`umin`	$\log_{10}$(minimum Re_x)
`umax`	$\log_{10}$(maximum Re_x)
`divdec`	divisions per decade of Re_x

Consequently, `umax`−`umin` decades of Re_x are computed with `divdec` evenly-spaced divisions per decade on a logarithmic scale. Since each computed Re_x implies a distance from the leading edge of the plate, these optional inputs cause `platelength` and `xpoints` to be ignored. From (11), the Stanton Number is computed from

$$C_H = \tfrac{1}{2} R_f c_f \tag{24}$$

for each correlation. The resulting C_H for each Re_x are then the only outputs printed in the Tecplot file `zpgout.tec`

```
                    * * * FLAT PLATE * * *

 Mach Num.   Re/x[1/m]   D[kg/m^3]    StatT[K] LAdWallT[K] TAdWallT[K]

     8.000   1.362E+06   8.426E-03       236.5      2439.0      2552.1


                     Local cf, delta_nu = nu_wall/u_tau and q_dot
                     --------------------------------------------

                                                RefTempMethod
                                              1. Eckert (1955)

           x =  1.000  Van Driest    Spalding   Lam Ref.T   Tur Ref.T

           T_wall [K]       300.0       300.0       300.0       300.0

                  F_c       2.581       2.581       3.183       3.289
                F_Rex       0.321       1.712       0.131       0.123
                Rex_i   4.377E+05   2.331E+06   1.779E+05   1.679E+05
               T* [K]        ---         ---       752.785     777.672

                   cf   1.707E-03   1.222E-03   4.945E-04   1.623E-03

          delta_nu [m]   3.427E-05   4.051E-05   6.368E-05   3.515E-05

          qdot [W/m^2]   5.222E+04   3.737E+04   1.618E+04   4.963E+04


                     Total heat transfer rate per unit plate width
                     ---------------------------------------------

           x =  1.000  Van Driest    Spalding   Lam Ref.T   Tur Ref.T

           Qdot [W/m]   6.533E+04   4.675E+04   2.866E+04   6.209E+04


                    Radiation and wall heat transfer rates: Case 0
                    ----------------------------------------------

                    User input: wall temperature [K] =  300.0

           x =  1.000  Van Driest    Spalding   Lam Ref.T   Tur Ref.T

          qr_dot [W/m]   0.000E+00   0.000E+00   0.000E+00   0.000E+00

          qw_dot [W/m]   5.222E+04   3.737E+04   1.618E+04   4.963E+04
```

Figure 4: Output file `zpgout.txt` from `zpg_qdot` for Mach 8 flat plate.

3.3 Running `zpg_qdot` for wedges and cones

Compressible flow past a wedge or cone at zero incidence usually results in an attached shock-wave and a zero-surface-pressure-gradient flow; see Bertin (1994, p. 356) and White (1974, p. 647). The correlation methods used for flat plates may then be applied behind the attached shock (although a slight modification is required for the three-dimensional cone flow).

The first step in running `zpg_qdot` for a wedge or cone is to determine the shock-wave angle to the vertical in radians. This is an input after `SHCK` in the `cmpexp` input file `1ns`. If a perfect gas with $\gamma = 1.4$ is assumed, then the shock-wave angles can be determined from NACA (1953, chart 2 for wedges and chart 5 for cones) or Sims (1964, table 11 for cones). For instance, for a 10° semi-angle wedge at Mach 8 and an altitude of 35 km, the shock-wave angle 15.5° to the horizontal obtained from NACA (1953, chart 2) is equivalent to 1.300 radians to the vertical; this is the `SHCK` input in the file `1ns` shown in figure 2.

The second step in running `zpg_qdot` for a wedge or cone is to change the value of `runcase` in the `zpg_qdot` input file `1ns_zpg`. Here `runcase = 1` for a wedge and `runcase = 2` for a cone. As before, the code is executed using the command `./.zpg_run`. The choice `runcase = 1` causes `zpg_qdot` to use the conditions behind the shock-wave as the free-stream parameters in the local skin friction and heat transfer rate calculations. The choice `runcase = 2` for the cone also causes the use of reference conditions behind the shock. However, to account for three-dimensional effects in a cone flow, the local skin friction coefficient is multiplied by factors of $\sqrt{3}$ and 1.176 for laminar and turbulent boundary layers respectively (White, 1974, p. 648).

3.4 Calculation of radiation and wall heat transfer rates

Radiation and wall heat transfer was implemented as an option in `zpg_qdot`. The local radiation heat transfer rate in the code is

$$\dot{q}_r = \epsilon\sigma(T_w^4 - T_\infty^4), \tag{25}$$

where $0 \leqslant \epsilon \leqslant 1$ is the emissivity, $\sigma = 5.669 \times 10^{-8}$ $\mathrm{Wm^{-2}K^{-4}}$ is the Stefan-Boltzmann constant, and T_∞ is the far-field temperature to which the body radiates. The local heat transfer rate through the wall is

$$\dot{q}_w = \frac{k_{\mathrm{wall}}}{d_{\mathrm{wall}}}(T_w - T_{\mathrm{back}}), \tag{26}$$

where k_{wall} is the wall conductivity, d_{wall} is the wall thickness, and T_{back} is the temperature of the back of the wall. The local convection heat transfer rate is then

$$\dot{q} = \dot{q}_r + \dot{q}_w. \tag{27}$$

The method used to calculate the local heat transfer rates $\dot{q}$, $\dot{q}_r$ and $\dot{q}_w$ depends on the data available. Three specific cases are now discussed for certain subsets of the parameters listed in table 2.

		Default if not entered
T_w	`T_wall`	–
T_∞	`T_infinity`	300 K
ϵ	`emissivity`	0.0
$\dot{q}_w$	`qw_dot`	–
d_{wall}	`d_wall`	–
k_{wall}	`k_wall`	–
T_{back}	`T_back`	–
Δ_{stop}	`Delta_stop`	0.1 K

Table 2: Optional radiation and wall heat transfer input parameters and their equivalents in the file `1ns_zpg`.

Case 1: User inputs T_w and ϵ in `1ns_zpg`

The local convection and radiation heat transfer rates can be determined directly from (12) and (25) respectively. From (27), the local wall heat transfer rate is $\dot{q}_w = \dot{q} - \dot{q}_r$. If ϵ is not entered and T_w is the only input (referred to as 'case 0'), then it is assumed that $\dot{q}_r = 0$, and $\dot{q}_w = \dot{q}$.

For cases 0 and 1, the optional additional entry of any two of the three wall properties d_{wall}, k_{wall} and T_{back} causes calculation and output of the third.

Case 2: User inputs $\dot{q}_w$ and ϵ in `1ns_zpg`

Here the wall temperature T_w is not known, and must be evaluated iteratively. Substitution of (25) into (27) and solving for T_w yields

$$T_w = \left(\frac{\dot{q} - \dot{q}_w}{\epsilon \sigma} + T_\infty^4 \right)^{1/4}. \tag{28}$$

An initial guess for the wall temperature $T_{w,0} = 300$ is made. The local convection heat transfer rate $\dot{q}_0$ can then be computed from $T_{w,0}$ using (12). Then, using (28), a new wall temperature $T_{w,1}$ can be computed. This procedure is continued until

$$|T_{w,i} - T_{w,i-1}| < \Delta_{\text{stop}}, \tag{29}$$

where Δ_{stop} is a pre-set stopping criterion. Once T_w is determined, the local radiation heat transfer rate can be calculated from (25). Radiation equilibrium cases can be computed by entering $\dot{q}_w = 0$ for any non-zero emissivity.

Again, the optional additional entry of any two of the three wall properties d_{wall}, k_{wall} and T_{back} causes calculation and output of the third.

Case 3: User inputs ϵ and wall properties $T_{\mathbf{back}}$, $k_{\mathbf{wall}}$ and $d_{\mathbf{wall}}$ in `1ns_zpg`

Here there are three unknowns T_w, $\dot{q}_r$ and $\dot{q}_w$, and three equations (25–27). Once again, the wall temperature must be evaluated iteratively. Substitution of (25) and (26) into (27) and solving for T_w yields

$$T_w = \left(\frac{\dot{q} - \dfrac{k_{\text{wall}}}{d_{\text{wall}}}(T_w - T_{\text{back}})}{\epsilon\sigma} + T_\infty^4 \right)^{1/4} . \tag{30}$$

The iterative procedure used is different to the one described for case 2 because T_w appears on both sides of (30). First, an initial guess for the wall temperature $T_{w,0} = 300$ is made. The local convection heat transfer rate $\dot{q}_0$ can then be computed from $T_{w,0}$ using (12). A new wall temperature $T_{w,1}$ can be computed from (30) using fixed-point iteration. This procedure is continued until

$$|T_{w,i} - T_{w,i-1}| < \Delta_{\text{stop}}, \tag{31}$$

where Δ_{stop} is a pre-set stopping criterion. Once T_w is determined, the local radiation and wall heat transfer rates can be calculated from (25) and (26).

Figure 5 shows an example radiation case 3 `1ns_zpg` input file for a Mach 8 flat plate at an altitude of 35 km. Here it is assumed that the surface has $\epsilon = 0.9$, and has wall properties $d_{\text{wall}} = 0.01\,\text{m}$, $T_{\text{back}} = 300\,\text{K}$, and $k_{\text{wall}} = 0.25\,\text{W m}^{-1}\text{K}^{-1}$. The corresponding output file `zpgout.txt` is shown in figure 6.

```
&ZPG_QDOT_PARAMETERS       emissivity = 0.90,
                          T_infinity = 300.0
                              d_wall = 0.010,
                              T_back = 500.0
                              k_wall = 0.250
                          Delta_stop = 0.1,
                         platelength = 1.0,
                             xpoints = 20,
                           shockcase = 0,
                        RefTempMethod = 1,
                              prandtl = 0.72,
               Reynolds_analogy_factor = 1.1 /
```

Figure 5: Input file `1ns_zpg` for `zpg_qdot` for Mach 8 flat plate radiation case 3.

```
                    * * * FLAT PLATE * * *

Mach Num.   Re/x[1/m]   D[kg/m^3]    StatT[K] LAdWallT[K] TAdWallT[K]

    8.000   1.362E+06   8.426E-03       236.5      2439.0      2552.1


                     Local cf, delta_nu = nu_wall/u_tau and q_dot
                     --------------------------------------------

                                                RefTempMethod
                                              1. Eckert (1955)

          x =  1.000  Van Driest    Spalding   Lam Ref.T   Tur Ref.T

          T_wall [K]       859.1       821.8       662.5       833.1

                 F_c       3.620       3.557       3.950       4.416
               F_Rex       0.104       0.281       0.089       0.072
               Rex_i   1.410E+05   3.830E+05   1.206E+05   9.805E+04
              T* [K]      ---         ---         934.039     1044.229

                  cf   1.527E-03   1.272E-03   4.840E-04   1.346E-03

        delta_nu [m]   1.358E-04   1.404E-04   1.732E-04   1.389E-04

        qdot [W/m^2]   3.636E+04   3.091E+04   1.348E+04   3.250E+04


                     Total heat transfer rate per unit plate width
                     ---------------------------------------------

          x =  1.000  Van Driest    Spalding   Lam Ref.T   Tur Ref.T

          Qdot [W/m]   4.548E+04   3.866E+04   2.388E+04   4.066E+04


                    Radiation and wall heat transfer rates: Case 3
                    ----------------------------------------------

                    User input: emissivity =  0.900
                    User input: T_back [K] =  500.0
                    User input: k_wall [W/mK] =    2.500E-01
                    User input: d_wall [m] =    1.000E-02

          x =  1.000  Van Driest    Spalding   Lam Ref.T   Tur Ref.T

        qr_dot [W/m]   2.738E+04   2.286E+04   9.419E+03   2.417E+04

        qw_dot [W/m]   8.977E+03   8.046E+03   4.064E+03   8.329E+03
```

Figure 6: Output file `zpgout.txt` from `zpg_qdot` for Mach 8 flat plate radiation case 3.

4 Comparison of engineering correlations with CFD and experiment

4.1 Goyne *et al.* (2003) high-enthalpy hypersonic boundary layers

Goyne, Stalker & Paull (2003) reported Stanton Numbers and skin-friction coefficients measured in hypersonic high-enthalpy laminar, transitional and turbulent boundary layers. Their experiments were performed in a free-piston shock tunnel with Mach Number, stagnation enthalpy and Reynolds Number in the ranges 4.4–6.7, 3–13 MJkg^{-1} and 0.16×10^6–21×10^6 respectively. The wall temperature in the experiments was approximately 300 K. Table 3 summarizes the average test-section conditions from the Goyne *et al.* (2003) experiments. Cases A, B and C are nominally laminar or transitional, and cases DHKQ, FILR and GJM are nominally transitional or turbulent.

Condition	T (K)	P (kPa)	ρ ($\mathrm{kg\,m^{-3}}$)	u ($\mathrm{m\,s^{-1}}$)	M_e	$Re_u \times 10^6$ ($\mathrm{m^{-1}}$)	h_0 ($\mathrm{MJ\,kg^{-1}}$)
A	486	0.87	0.0063	2800	6.4	0.669	4.4
B	772	1.03	0.0045	3460	6.2	0.434	7.8
C	1010	2.70	0.0090	3740	5.9	0.789	9.1
DHKQ	336	8.14	0.0842	2425	6.6	10.1	3.2
FILR	741	10.9	0.0499	3240	6.0	4.65	6.2
GJM	1147	10.1	0.0294	3783	5.7	2.45	9.0

Table 3: Goyne *et al.* (2003) average test conditions.

The program `zpg_qdot` was run for each case listed in table 3. An isothermal wall temperature $T_w = 300\,\mathrm{K}$ was used, and $Pr = 0.72$ and $R_f = 1.0$. Stanton Numbers were computed for Reynolds Numbers based on the distance from the leading edge of the flat plate in the range 10^5–10^8, with 10 divisions per decade of Re_x. The input files `1ns` and `1ns_zpg` and the resulting summary output file `zpgout.txt` can be found in Appendix A.

CFD was also carried out for each of the cases listed in table 3. Laminar calculations were performed for cases A, B and C, while both the k–ω and Menter-SST turbulence models were used in cases DHKQ, FILR and GJM. The details of the CFD inputs and grids can be found in Appendix A. The Stanton Number was computed from the CFD data using a program written by the author called `plotprof2`. This program implemented the definition (7) to obtain

$$C_H = \frac{\dot{q}}{\rho_e u_e (h_{aw} - h_w)}. \tag{32}$$

Here h_{aw} was computed using (8) with a recovery factor defined by (10a) or (10b), and a

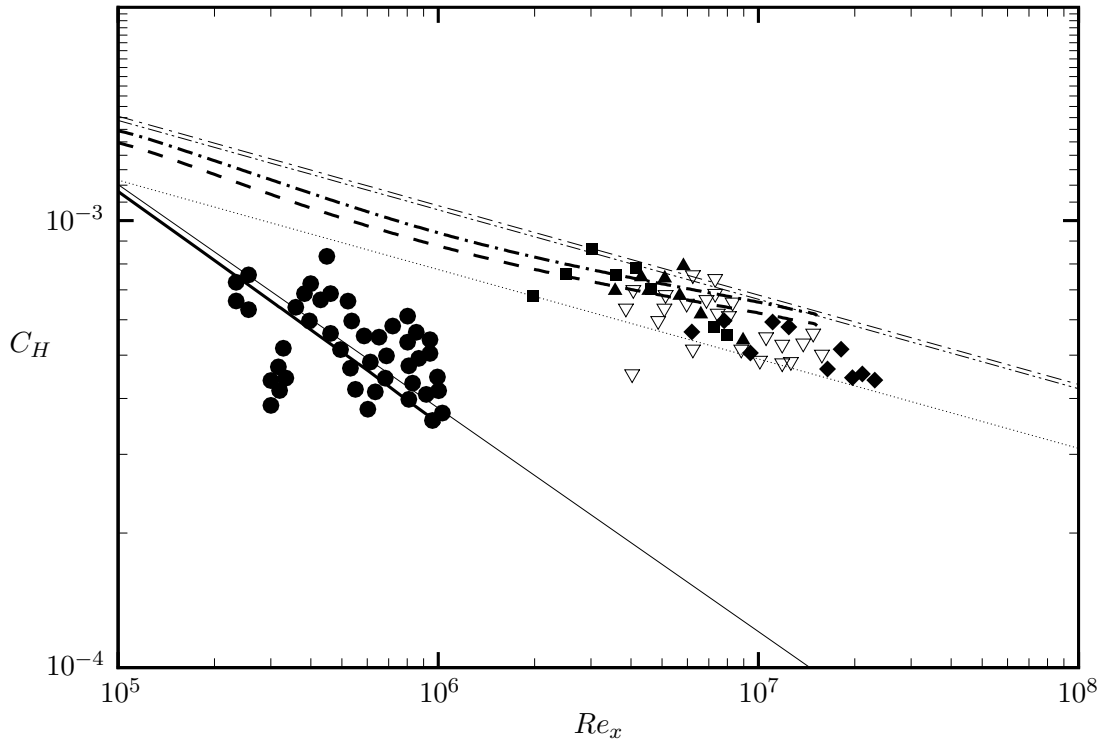

Figure 7: Stanton Number from engineering correlations implemented in `zpg_qdot` and CFD results compared to experimental data from Goyne *et al.* (2003) for $3.5\,\mathrm{MJ\,kg^{-1}}$ nominal stagnation enthalpy. A Reynolds analogy factor $R_f = 1.0$ was used to calculate the Stanton Number from the experimental data and engineering correlations.

Prandtl Number $Pr = 0.72$. The local heat transfer rate was computed using

$$\dot{q} = k_w \left[\frac{\partial T}{\partial y}\right]_{y=0}, \tag{33}$$

where k_w is the conductivity of the fluid at the wall. From the definition of the Prandtl Number (9),

$$k_w = \frac{\gamma_w}{\gamma_w - 1}\frac{p_w \mu_w}{\rho_w T_w Pr}, \tag{34}$$

where γ_w, p_w, μ_w and ρ_w are the ratio of specific heats, static pressure, dynamic viscosity and static density of the fluid at the wall respectively obtained from the CFD data.

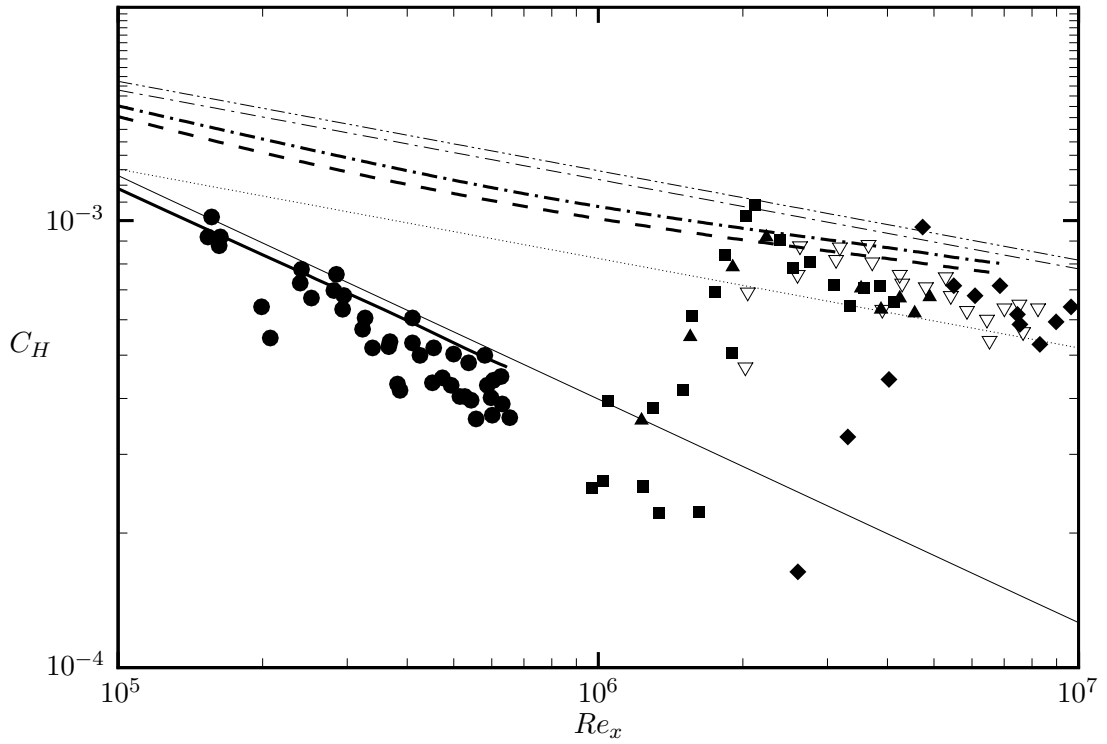

Figure 8: Stanton Number from engineering correlations implemented in `zpg_qdot` and CFD results compared to experimental data from Goyne *et al.* (2003) for 6.5 MJ kg^{-1} nominal stagnation enthalpy. A Reynolds analogy factor $R_f = 1.0$ was used to calculate the Stanton Number from the experimental data and engineering correlations.

Figure 7 shows the present engineering correlation and CFD results compared to the Goyne *et al.* (2003) data for a nominal stagnation enthalpy of 3.5 MJ kg^{-1}. The laminar engineering correlation and CFD results for case A agree very closely, with both curves passing through the centre of the cluster of experimental measurements. Among the turbulent engineering correlations, there is close agreement between the van Driest (1956) and Eckert (1955) methods, with both passing through the upper limits of the experimental measurements. The Spalding & Chi (1964) method provides a somewhat lower estimate of C_H, so that the turbulent engineering correlations roughly bracket the experimental data. The turbulent CFD results fall between the upper and lower estimates of the correlations, passing approximately through the middle of the measurements. It is also notable that the Menter-SST model predicts a slightly larger C_H compared with the k–ω model.

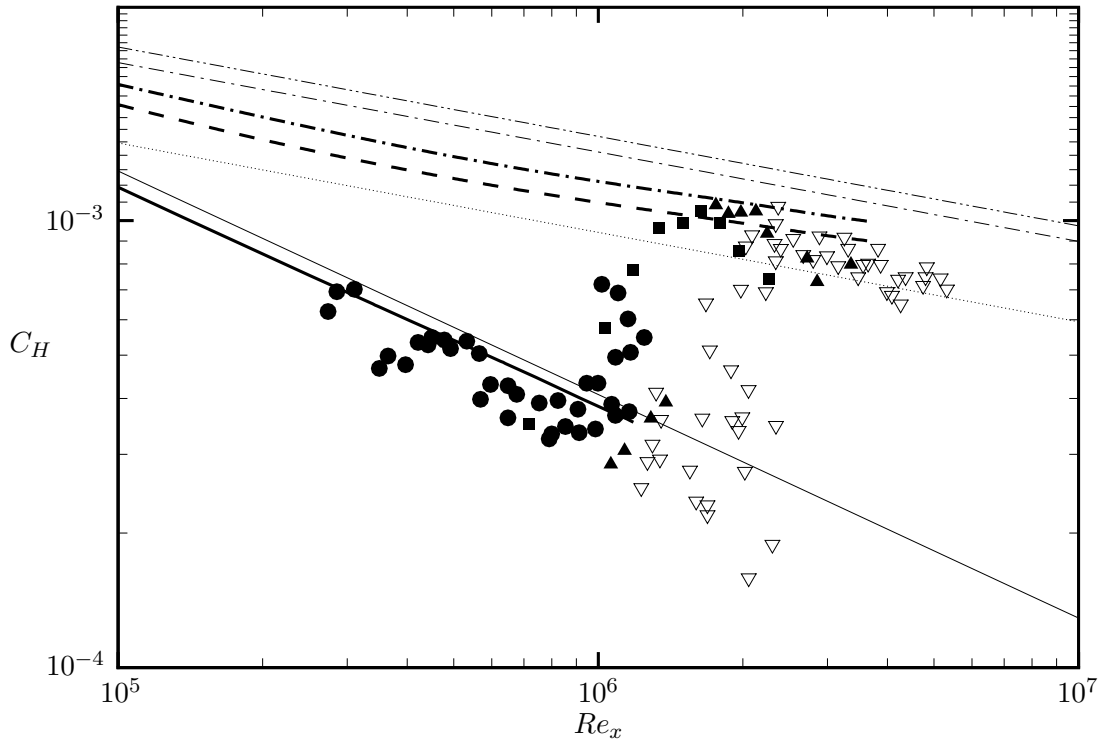

van Driest (1956)			
Eckert (1955)	Symbol	Condition	$Re_u \times 10^6$ (m^{-1})
Spalding & Chi (1964)	●	C	0.79
Eckert (1955) (laminar)	■	G	1.5
CFD (laminar)	▲	J	2.3
CFD (k–ω)	▽	M	3.5
CFD (Menter-SST)			

Figure 9: Stanton Number from engineering correlations implemented in `zpg_qdot` and CFD results compared to experimental data from Goyne *et al.* (2003) for 9.0 MJ kg^{-1} nominal stagnation enthalpy. A Reynolds analogy factor $R_f = 1.0$ was used to calculate the Stanton Number from the experimental data and engineering correlations.

Figure 8 shows the present engineering correlation and CFD results compared to the Goyne *et al.* (2003) data for a nominal stagnation enthalpy of 6.5 MJ kg^{-1}. Here the experimental data shows transition for Re_x roughly in the range 1×10^6–2×10^6. As before, the laminar engineering correlation and CFD results agree very closely. In this case, however, the curves pass through the upper limits of the laminar experimental measurements. Among the turbulent correlations, there is again close agreement between the van Driest (1956) and Eckert (1955) methods. As expected, the Spalding & Chi (1964) method yields a lower estimate of C_H, so that the turbulent engineering correlations roughly bracket the data for $Re_x > 2 \times 10^6$. Again, the turbulent CFD results fall between the upper and lower estimates of the correlations, with the Menter-SST model predicting a slightly larger C_H compared with the k–ω model.

Figure 9 shows the present engineering correlation and CFD results compared to the Goyne *et al.* (2003) data for a nominal stagnation enthalpy of $9.0\,\mathrm{MJ\,kg^{-1}}$. Transition is again evident in the experimental data for Re_x roughly in the range 1×10^6–2×10^6. The laminar correlation and CFD results are almost unchanged from those previously shown in figure 8, although the separation between the two curves is slightly larger. As before, both curves pass through the upper limits of the laminar experimental measurements. However, the Stanton Numbers predicted by the turbulent correlations are somewhat larger than the previous results shown in figure 8. The van Driest (1956) and Eckert (1955) curves lie above all of the experimental data points, while the Spalding & Chi (1964) curve passes through the lower limits of the turbulent experimental data for $Re_x > 2 \times 10^6$. As before, the turbulent CFD results fall between the upper and lower estimates of the correlations.

As mentioned earlier, the correlation and CFD methods do not model transition. It is always assumed that the origin of a turbulent boundary layer is at the leading edge of the plate. Therefore, it might be expected that the turbulent correlations and CFD would tend to under-predict the Stanton Number. If this is the case, why do the turbulent correlations and CFD data in figures 7–9 show reasonable agreement with the turbulent experimental data? In answering this question, it might be useful to conduct a thought experiment in which two turbulent Stanton Number profiles are compared. First, assume that the boundary layer origin for the first profile is at the leading edge of the plate, and for the second profile it is somewhat upstream of the point of transition. Much further downstream (at large values of Re_x, just like the data plotted on logarithmic scales in figures 7–9), the relatively small difference in location of boundary layer origin for the two profiles is likely to be unimportant. Therefore, there might be little difference between the two Stanton Number profiles at such a downstream location on a logarithmic scale. A transition model much further upstream would then be expected to have only a small impact in this situation. It should also be noted that Goyne *et al.* (2003, §6.3) infers that their boundary layers had insufficient length to fully relax from a transitional to a turbulent state. The measured Stanton Numbers would then be somewhat smaller than those expected from a turbulent boundary layer, thereby offsetting the absence of a transition model in the correlations and CFD.

Another reason why the van Driest (1956) and turbulent Eckert (1955) correlations show reasonable agreement with the experimental data is that they have a tendency to over-predict skin-friction and heat transfer on cold walls, which further compensates for the absence of transition. (Presently, $T_w/T_0 < 0.1$ in all cases). This over-prediction effect was observed by Holden (1972) in a series of high-stagnation-enthalpy shock tunnel experiments in the Mach 7–10 range. Additionally, the turbulent correlation results depend on the choice of the Reynolds analogy factor. Presently $R_f = 1.0$ based on the Goyne *et al.* (2003) experimental data, but the choice, for example, of a slightly smaller value would improve agreement between the van Driest (1956) and turbulent Eckert (1955) correlations and the experimental data.

On the other hand, the CFD results were obtained directly from the wall-normal temperature gradient without use of a Reynolds analogy. The implied Reynolds analogy factor $R_f = 2C_H/c_f$ was computed with the program `plotprof2` for comparison with the value $R_f = 1.0$ used in the experiment. For the k–ω turbulence model CFD runs DHKQ, FILR and GJM, R_f at the maximum Re_x was found to be 1.17 in all cases. This is 17% larger than the experimental value, and partly explains why the Stanton Numbers from the CFD cases are larger than what would be expected without a transition model.

4.2 Chien (1974) Mach 7.9 5° semi-angle cone

Chien (1974) reported skin-friction and heat-transfer measurements on a 5° semi-angle cone at a free-stream Mach Number of 7.9. The local Mach Number behind the shock and at the edge of the boundary layer was 7.15. Cooling was used to control the wall temperature of the cone, and measurements were made for ratios of wall temperature to stagnation temperature in the range 0.11–0.35. The experimental data was presented in the format $10^4 C_H$ versus $10^{-6} Re_x$ up to a maximum $Re_x = 21.7 \times 10^6$. Table 4 summarizes the average test-section conditions from the Chien (1974) experiments.

T_w/T_0	P_0 (MPa)	T_0 (K)	$Re_u \times 10^6$ (m^{-1})	T_w (K)
0.35	13.128	814	30.68	288
0.20	15.072	808	35.79	158
0.11	15.086	812	35.50	88

Table 4: Chien (1974) average test conditions.

The program `zpg_qdot` was run for each case listed in table 4, with $Pr = 0.72$ and $R_f = 1.0$. The cone surface was 0.60 m in length, and Stanton Numbers were computed for Reynolds Numbers based on the distance from the leading edge of the cone. In each case, an isentropic expansion from the stagnation conditions listed in table 4 was used to establish the free-stream conditions used to compute the unit Reynolds Number. This was followed by an oblique shock at 8.8226° to the horizontal, or 1.4168 radians to the vertical, obtained from Sims (1964, table 11). The pressure ratio for the isentropic expansion was chosen so that the Mach Number after passage through the shock was 7.15. Table 5 summarizes these flow properties. (It should be noted in this table that $M_1 \approx 7.5$ was somewhat lower than the experimental free-stream Mach Number of 7.9) The input files `1ns` and `1ns_zpg` and the resulting summary output file `zpgout.txt` used in these calculations can be found in Appendix B.

T_w/T_0	P_1/P_0	P_1 (kPa)	T_1 (K)	M_1	$Re_{u1} \times 10^6$ (m^{-1})	P_2 (kPa)	T_2 (K)	M_2	$Re_{u2} \times 10^6$ (m^{-1})
0.35	1.505×10^{-4}	1.98	68.7	7.52	26.8	2.73	75.2	7.15	30.4
0.20	1.470×10^{-4}	2.22	68.0	7.53	30.6	3.07	74.6	7.15	34.7
0.11	1.470×10^{-4}	2.22	68.4	7.53	30.3	3.07	75.0	7.15	34.5

Table 5: Isentropic expansion and properties behind shock computed by `zpg_qdot` for the Chien (1974) cone cases. The subscript 1 refers to flow properties after an isentropic expansion with pressure ratio P_1/P_0 from the stagnation conditions listed in table 4. The subscript 2 refers to flow properties after passing through the attached oblique cone shock at 8.8226° to the horizontal, or 1.4168 radians to the vertical, which was obtained from Sims (1964, table 11). The pressure ratio was chosen so that $M_2 = 7.15$ behind the shock.

Difficulties were encountered in the `zpg_qdot` calculations owing to the low free-stream static temperatures. These were outside the valid range allowed by the routine inside `cmpexp` used to compute the dynamic viscosity. As an alternative, the dynamic viscosity μ at temperature T was evaluated independently in the code `zpg_qdot` using Sutherland's law (Anderson, 1989, p. 242). Here

$$\mu = \mu_{\text{ref}} \left(\frac{T}{T_{\text{ref}}} \right)^{3/2} \frac{T_{\text{ref}} + S}{T + S}, \tag{35}$$

where for air $\mu_{\text{ref}} = 1.789 \times 10^{-5}\,\text{kg}\,\text{m}^{-1}\,\text{s}^{-1}$, $T_{\text{ref}} = 288\,\text{K}$ and $S = 110\,\text{K}$.

Laminar and turbulent CFD was also carried out for each of the cases listed in table 4. Both the k–ω and Menter-SST turbulence models were used. The details of the CFD can be found in Appendix B. The Stanton Number was computed from the CFD data using the program `plotprof2`. It should be noted that the unit Reynolds Number used to determine Re_x was computed from the properties of the free stream, whereas the Stanton Number was computed using the fluid properties behind the cone shock.

Figure 10 shows the engineering correlation and CFD results compared to the Chien (1974) data for $T_w/T_0 = 0.35$. Transition is evident in the experiment for Re_x roughly in the range 5×10^6–10×10^6. The laminar CFD result agrees quite closely with the experimental data for $Re_x < 3 \times 10^6$, whereas the laminar engineering correlation result somewhat under-predicts the Stanton Number in this range. There is reasonable agreement among the turbulent engineering correlation and CFD results, but these all lie below the cluster of turbulent experimental data points for $Re_x > 10 \times 10^6$. This is exactly what would be expected when data is plotted on a linear scale in the absence of a transition model (compare with the figures using logarithmic scales in section 4.1). The Reynolds analogy factor for the turbulent CFD k–ω model computed with `plotprof2` was $R_f = 1.17$, in good agreement with the Goyne *et al.* (2003) flat plate result obtained in section 4.1. One other point of interest is that the turbulent Eckert (1955) and Spalding & Chi (1964) correlations agree closely, while van Driest (1956) predicts a somewhat larger Stanton Number.

Figures 11 and 12 show the engineering correlation and CFD results compared to the Chien (1974) data for $T_w/T_0 = 0.20$ and 0.11 respectively. Fewer experimental data points are available for comparison in these colder-wall cases, but transition is again evident in the experiment for Re_x roughly in the range 5×10^6–10×10^6. Again, the laminar CFD result lies slightly above the laminar correlation in both cases, and both curves fall within 20% of the few available laminar experimental data points. However, comparing the laminar CFD and correlation curves from figures 10–12 shows that their amplitudes are almost unaffected by the decreasing wall temperature. On the other hand, the Stanton Numbers from the turbulent CFD steadily increase as the wall temperature falls, yielding quite reasonable agreement with the turbulent experimental data in figures 11 and 12. The Reynolds analogy factor for the k–ω turbulence model results was found to be 1.19 in both cases.

The behaviour of the turbulent correlations also changes with decreasing wall temperature. While the Eckert (1955) and Spalding & Chi (1964) curves showed close agreement in figure 10, the Eckert (1955) curve in figure 11 has moved closer to the van Driest (1956) result. Very close agreement between the Eckert (1955) and van Driest (1956) correlations

and the experimental data is then achieved in figure 12. Here, with $T_w/T_0 = 0.11$, good agreement with the experimental data is obtained because the van Driest (1956) and Eckert (1955) correlations tend to over-predict heat transfer on cold walls, thereby somewhat compensating for the absence of a transition model. It is notable that the Spalding & Chi (1964) curve falls much further below the other correlations and experimental data points. These are similar to the observations made about the Goyne *et al.* (2003) turbulent flat plate case DHKQ with $T_w/T_0 \approx 0.1$ shown in figure 7.

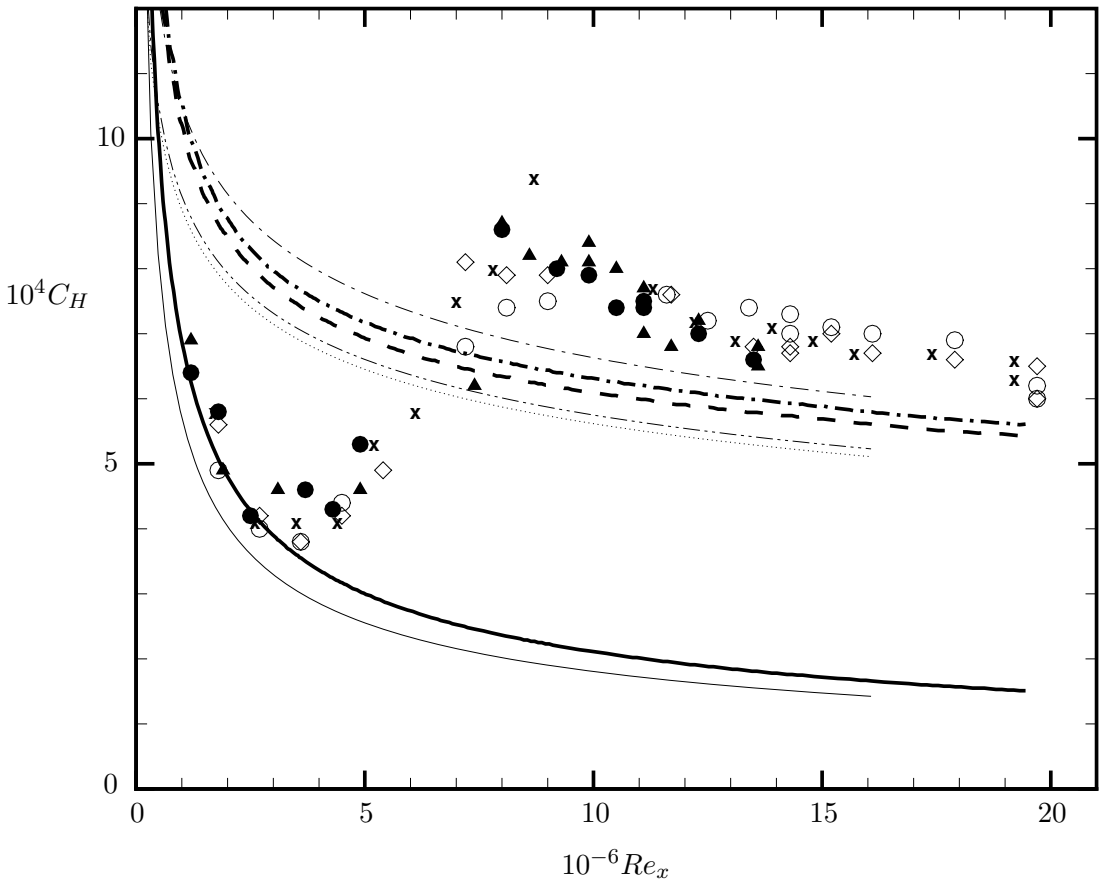

van Driest (1956)
Eckert (1955)
Spalding & Chi (1964)
Eckert (1955) (laminar)
CFD (laminar)
CFD (k–ω)
CFD (Menter-SST)

Symbol	Run	$Re_u \times 10^6$ (m^{-1})
○	21	35.2
×	23	34.3
◇	24	35.3
▲	26	24.3
●	29	24.3

Figure 10: Stanton Number from engineering correlations implemented in `zpg_qdot` and CFD results compared to experimental data from Chien (1974) for a Mach 7.9 laminar and turbulent 5° semi-angle cone boundary layer with $T_w/T_0 = 0.35$. A Reynolds analogy factor $R_f = 1.0$ was used to calculate the Stanton Number in the engineering correlations.

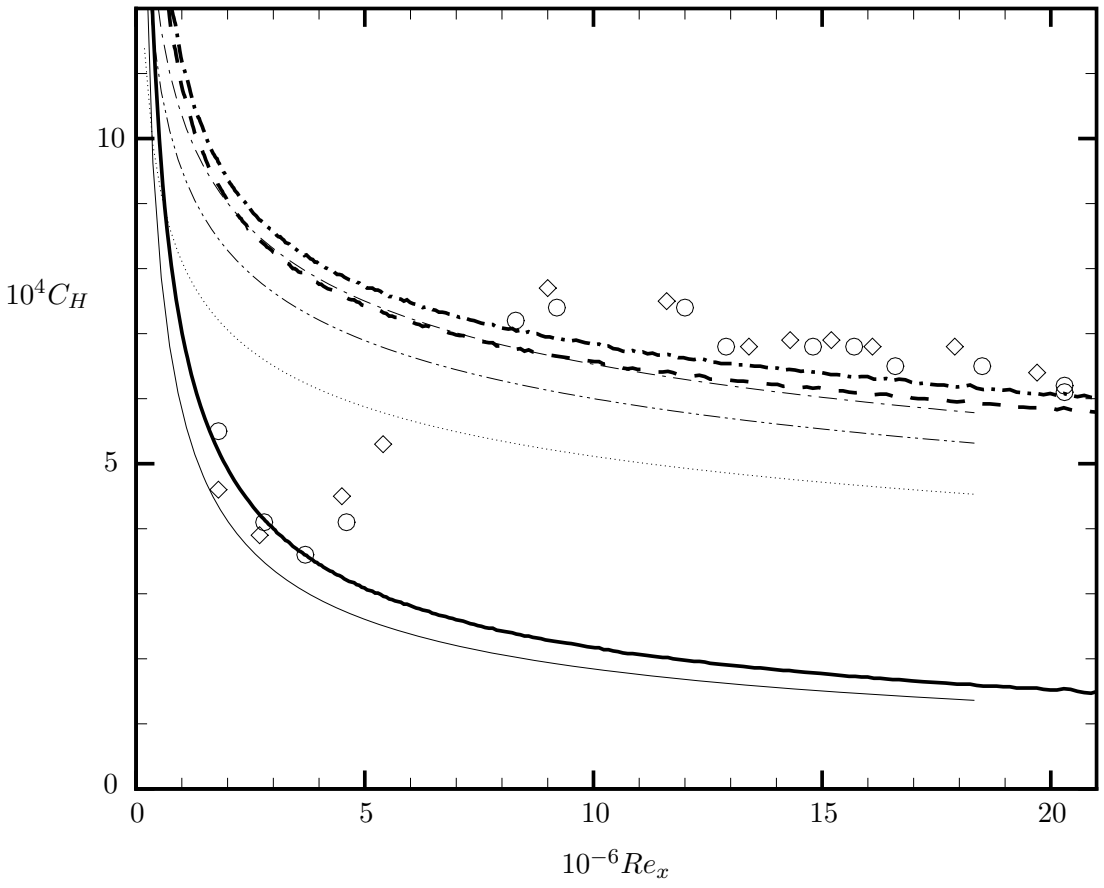

van Driest (1956)			
Eckert (1955)			
Spalding & Chi (1964)	Symbol	Run	$Re_u \times 10^6$ (m^{-1})
Eckert (1955) (laminar)	○	18	36.3
CFD (laminar)	◇	20	35.2
CFD (k–ω)			
CFD (Menter-SST)			

Figure 11: Stanton Number from engineering correlations implemented in `zpg_qdot` and CFD results compared to experimental data from Chien (1974) for a Mach 7.9 laminar and turbulent 5° semi-angle cone boundary layer with $T_w/T_0 = 0.20$. A Reynolds analogy factor $R_f = 1.0$ was used to calculate the Stanton Number in the engineering correlations.

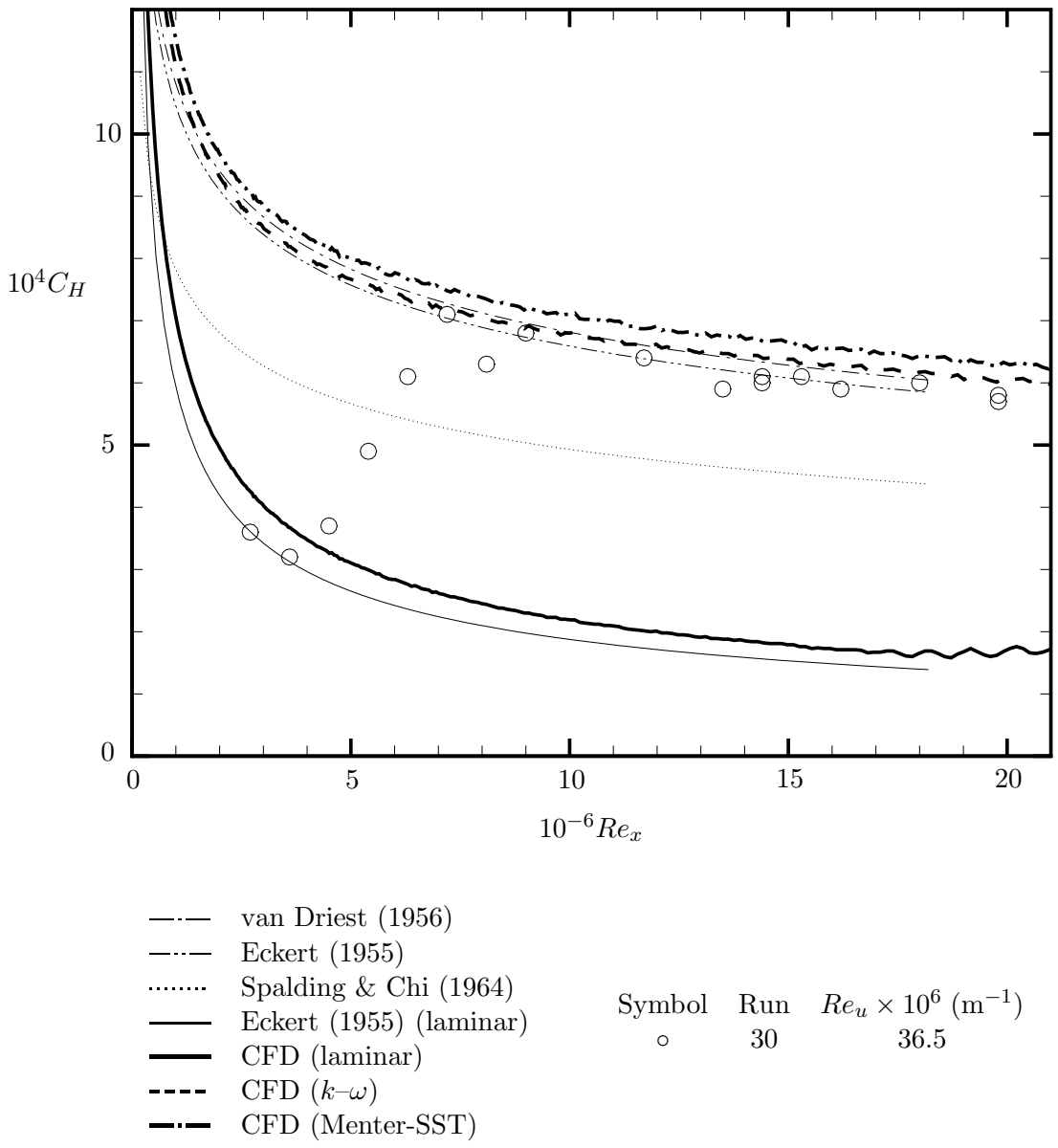

Figure 12: Stanton Number from engineering correlations implemented in `zpg_qdot` and CFD results compared to experimental data from Chien (1974) for a Mach 7.9 laminar and turbulent 5° semi-angle cone boundary layer with $T_w/T_0 = 0.11$. A Reynolds analogy factor $R_f = 1.0$ was used to calculate the Stanton Number in the engineering correlations.

4.3 Mach 8 flat plate, 10° wedge and cone at 35 km

In this section, local skin friction coefficients, viscous length scales and heat transfer rates are computed for a flat plate and a 10° semi-angle wedge and cone with wall temperature 300 K at Mach 8 and an altitude of 35 km. Here the engineering correlation results are compared with CFD data only. These particular flat plate, wedge and cone cases were selected for investigation because they provide some useful comparisons of heat transfer rates at a Mach Number and altitude that might be encountered in the HIFiRE flight test program.

The free-stream static temperature, density and pressure at an altitude of 35 km were determined using the program `atmos_alt` (which uses the 1976 US Standard Atmosphere Curve Fitter). This data is shown in table 6.

Free-stream Mach Number	8.0
Free-stream static temperature (K)	236.47
Free-stream static density (kg m^{-3})	0.0084629
Free-stream static pressure (Pa)	574.42

Table 6: Reference conditions at an altitude of 35 km for Mach 8 flat plate, 10° semi-angle wedge and cone cases.

The program `zpg_qdot` was run for the Mach 8 flat plate, 10° semi-angle wedge and cone cases using the free-stream conditions listed in table 6. In all cases, the wall temperature was 300 K, the surface length was 1.0 m and $Pr = 0.72$ and $R_f = 1.1$. For the 10° semi-angle wedge and cone, the shock angles obtained from NACA (1953, chart 2 and chart 5) were 1.300 and 1.344 radians to vertical respectively. The input files `1ns` and `1ns_zpg` and the resulting summary output file `zpgout.txt` used in these calculations can be found in Appendix C.

Laminar and turbulent CFD was also carried out for the Mach 8 flat plate cases, using both the k–ω and Menter-SST models in the turbulent cases. For the 10° semi-angle wedge and cone, turbulent CFD was carried out using the Menter-SST model only. The details of the CFD inputs and grids are listed in Appendix C. The resulting local skin friction coefficients, viscous length scales and heat transfer rates were computed using the program `plotprof2`.

Figure 13 shows a comparison of the CFD and correlation results for the local skin friction coefficient, viscous length scale and heat transfer rate as a function of distance from the leading edge of the Mach 8 flat plate. In the laminar case, the Eckert (1955) reference temperature method results overlap the CFD results almost exactly for c_f and $\dot{q}$, and only slightly over-estimate δ_ν. In the turbulent case, CFD results for the k–ω and Menter-SST turbulence models are compared to the three correlations. In all cases, the Menter-SST and k–ω curves overlap until about $x = 0.05$, at which point a noticeable 'kink' appears in the Menter-SST curves. It is interesting to note that there is about as much variability between the two turbulence models after this point as there is among some of the correlations. For c_f and $\dot{q}$, the van Driest (1956) and Eckert (1955) correlations match

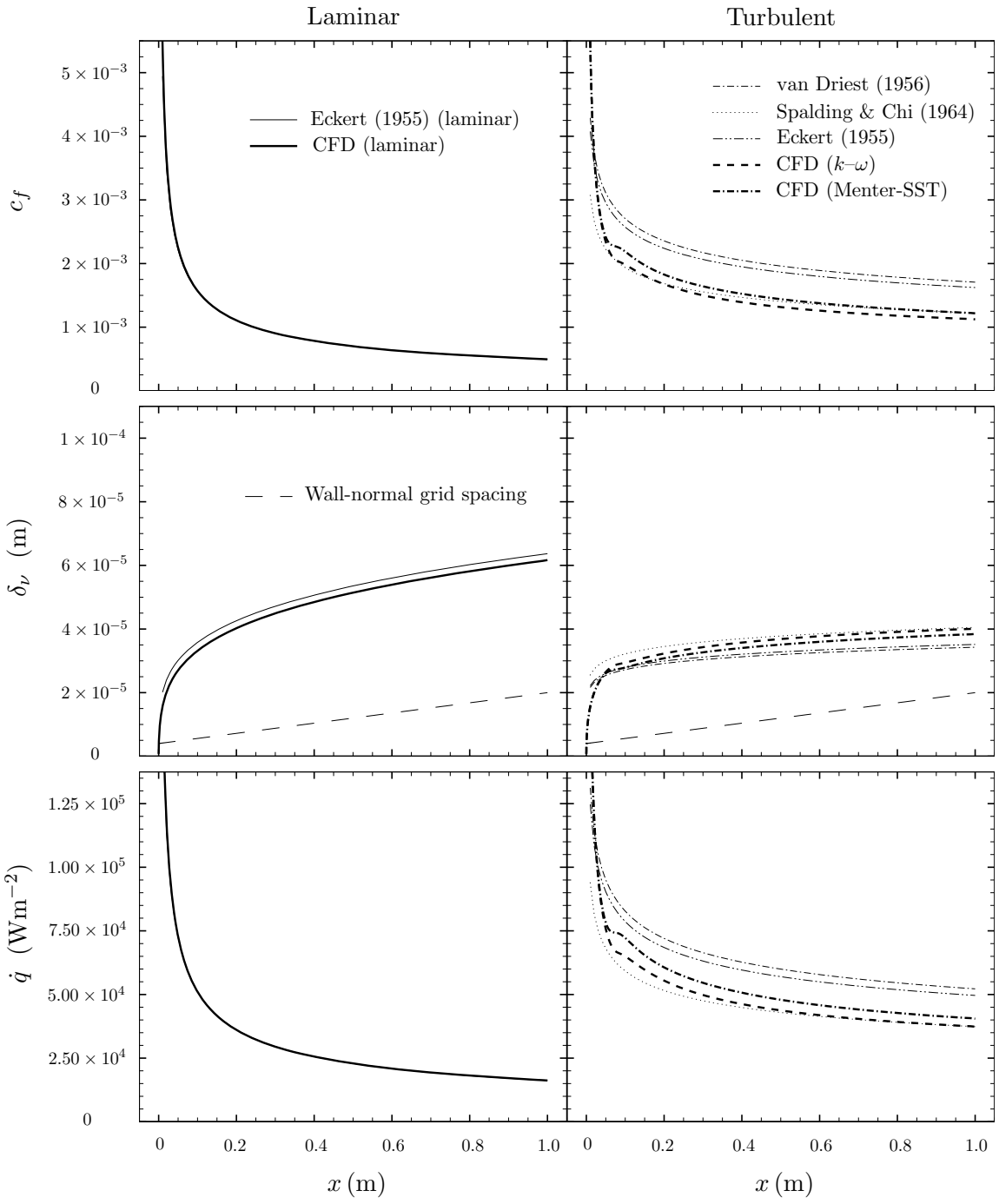

Figure 13: Local skin friction coefficient, viscous length scale and heat transfer rate as a function of distance x from the leading edge of a Mach 8 flat plate at an altitude of 35 km. The wall-normal grid spacing shown is the distance from the wall to the first grid point.

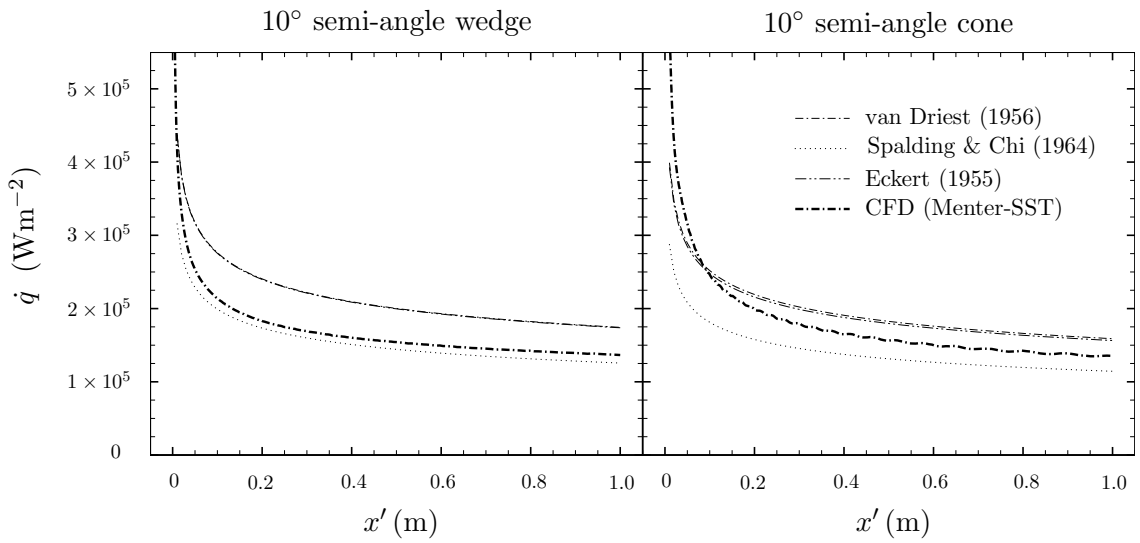

Figure 14: Local turbulent heat transfer rate $\dot{q}$ as a function of distance x' from the leading edge of a 10° semi-angle wedge (left) and cone (right) at Mach 8 and an altitude of 35 km. The Menter-SST turbulence model was used in both cases.

the CFD results quite well for $x < 0.025$, while the Spalding & Chi (1964) correlation shows better agreement for $x > 0.05$. For δ_ν, very good agreement among the correlations and CFD is obtained. This demonstrates that `zpg_qdot` would be a useful tool for determining wall-normal grid spacing for CFD in simple flat-plate cases. By comparison to the CFD results, the van Driest (1956) and Eckert (1955) correlations over-estimate $\dot{q}$ by about 30% in some cases. Nevertheless, since the CFD results fall between the upper and lower limits of the correlations, the overall agreement between the CFD and correlations is probably acceptable.

Figure 14 shows a comparison of the turbulent CFD and correlation results for the local heat transfer rate as a function of distance from the leading edge of the 10° semi-angle wedge and cone. For the wedge, there is close agreement between the CFD and Spalding & Chi (1964) correlation. The van Driest (1956) and Eckert (1955) correlations overlap, and predict somewhat larger local heat transfer rates. For the cone, the local heat transfer rates predicted by the correlations are slightly smaller than for the wedge. Compared with the local heat transfer rates obtained from the Mach 8 flat plate calculations, the present results are about 3.5 and 3.0 times larger for the wedge and cone respectively. The shape of the cone CFD curve is somewhat different to the wedge curve, where, compared with the correlations, the cone CFD over-estimates $\dot{q}$ close to the leading edge. Small oscillations also appear in the cone CFD curve, perhaps indicating that the result is not very satisfactory. This problem could stem from the small shock-wave angle, which was found to be only about 2.2° measured from the surface of the cone. Compared to the wedge, there is a stronger interaction between the boundary layer and this shock-wave in the cone CFD. The cone CFD was repeated on a finer grid with different node clustering, and this somewhat reduced the oscillations, but did not eliminate them. Similar oscillations were observed in the Chien (1974) Mach 7.9 5° cone CFD with $T_w/T_0 = 0.11$ shown in figure 12. Since $T_0 \approx 3260\,\mathrm{K}$ and $T_w/T_0 \approx 0.09$ in the present case, it is possible that the oscillations are associated with cold walls.

4.4 Total heat transfer rates for $5 \leqslant M_e \leqslant 10$ flat plates at 35 km

In addition to the local rate of heat transfer to a surface, the total rate of heat transfer might be considered during the design of a hypersonic vehicle. The total rate of heat transfer per unit flat plate width at distance x from the leading edge can be computed from (22), so that

$$\dot{Q}(x) = \int_0^x \dot{q}(x')\mathrm{d}x'. \tag{36}$$

Equations (23a–b) summarize how the program `zpg_qdot` computes $\dot{Q}$ from (22) using engineering correlations. The program outputs the result $\dot{Q}(x = \texttt{platelength})$ in the file `zpgout.txt`. This quantity is useful for comparing total heat transfer rates over a range of Mach Numbers.

Figure 15 shows a comparison of $\dot{Q}(1)$ computed using `zpg_qdot` to CFD results obtained by numerical integration of (22) for laminar and turbulent flat plate boundary layers respectively at an altitude of 35 km over the range $5 \leqslant M_e \leqslant 10$. These are a typical altitude and range of Mach Numbers that might be encountered by hypersonic vehicles in the HIFiRE flight test program. In the laminar case, the Eckert (1955) correlation somewhat under-estimates $\dot{Q}(1)$ compared with the CFD. In the turbulent case, the CFD results fall between the upper and lower predictions from the correlations. Although now slightly over-estimating the CFD results, the Eckert (1955) correlation provides the closest agreement with the CFD.

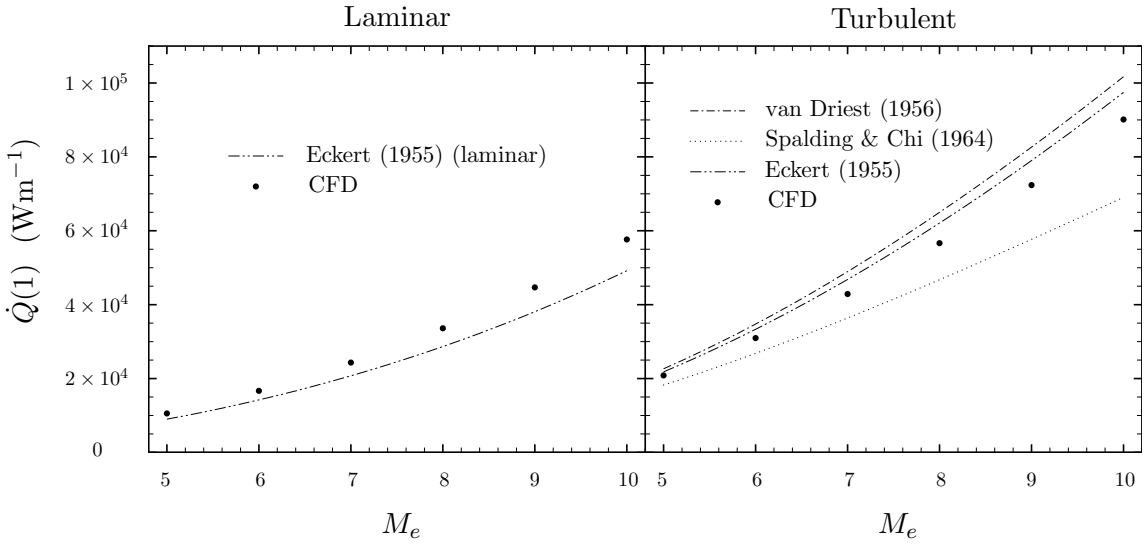

Figure 15: Total heat transfer rate per unit plate width at $x = 1$ m from the leading edge as a function of free-stream Mach Number for laminar (left) and turbulent (right) flat plate boundary layers at an altitude of 35 km. The Menter-SST turbulence model was used to compute the turbulent results.

4.5 Mach 5 and 6 vitiated air flat plate boundary layers

Vehicles travelling at hypersonic Mach Numbers experience very large surface heating rates owing to viscous dissipation in boundary layers and the high stagnation temperature and enthalpy of the fluid. Replicating these conditions in laboratory tests in continuous-flow wind tunnels is a significant problem. One way to achieve the high-stagnation-enthalpy conditions is the direct combustion of fuel in a wind tunnel stream. The resulting mixture of combustion products and oxygen-depleted air (known as vitiated air) is then expanded to a hypersonic velocity. The Propulsion Systems Branch of Air Vehicles Division has proposed the construction of such a facility at DSTO-Melbourne for the continuous-flow testing of hypersonic vehicles.

However, there are problems associated with the use of vitiated air in hypersonic wind-tunnel testing. The most obvious of these is the fact that combustion alters the chemical composition of the heated air flow. It is therefore important to understand how this affects the resulting local heat transfer rate to a surface immersed in the vitiated air flow. In particular, it would be useful to compare the local heat transfer rate for a flat plate in vitiated air at Mach Numbers achievable in the proposed DSTO-Melbourne facility with a flat plate in air at a Mach Number and altitude typical of HIFiRE flight tests. Therefore, in this section, local heat transfer rates for Mach 5 and 6 flat plates immersed in vitiated air are compared with results from the Mach 8 flat plate at 35 km discussed earlier in §4.3. Engineering correlations and CFD will be used to compute the local heat transfer rates.

Table 7 lists the vitiated air species mass fractions expected in the proposed DSTO-Melbourne continuous-flow hypersonic wind tunnel. These mass fractions were extracted from a `cmpexp` input file called `cmex_rawin.txt` computed by Dr. Nigel Smith. It is now assumed that the vitiated air is expanded isentropically to Mach 5 and 6 from the stagna-

Specie	Mass fraction
CH4	0.24253E-20
H2	0.47259E-05
H	0.30449E-06
O	0.12847E-03
OH	0.15584E-02
HO2	0.21454E-04
H2O2	0.14615E-05
H2O	0.89410E-01
C	0.32268E-20
CO	0.17339E-03
CO2	0.11001E+00
CH	0.51399E-21
CH2	0.15742E-20
CH3	0.71385E-20
HCO	0.10506E-10
CH2O	0.22823E-12
CH2OH	0.60038E-18
CH3OH	0.24977E-19
O2	0.23048E+00
N2	0.56821E+00

Table 7: Species mass fractions for Mach 5 and 6 vitiated air flat plate boundary layers.

tion pressure, temperature and density of 3 MPa, 2204 K and 4.6697 kg m^{-3} respectively. This expansion was computed with `cmpexp` as part of each `zpg_qdot` run. The input files `1ns` and `1ns_zpg` and the resulting summary output file `zpgout.txt` used in these calculations can be found in Appendix D. Table 8 lists the static properties of the vitiated air after the isentropic expansions. The Mach Number M_1, static temperature T_1 and static density ρ_1 listed in this table were the reference conditions used in the vitiated flat plate CFD calculations.

P_1/P_0	M_1	P_1 (kPa)	T_1 (K)	ρ_1 (kg m^{-3})	$Re_{u1} \times 10^6$ (m^{-1})
1.15×10^{-3}	5.00	3.45	460	2.57×10^{-2}	2.27
3.50×10^{-4}	6.00	1.05	335	1.08×10^{-2}	1.27

Table 8: Properties of vitiated air after isentropic expansion to Mach 5 and 6. The subscript 1 refers to flow properties after an isentropic expansion with pressure ratio P_1/P_0 from the stagnation conditions listed in the text above.

Figures 16–18 show comparisons of the local heat transfer rate for Mach 5 and 6 vitiated air turbulent flat plate boundary layers with a Mach 8 flat plate at an altitude of 35 km for the van Driest (1956), Eckert (1955), and Spalding & Chi (1964) correlations. An isothermal wall temperature $T_w = 300$ K was assumed in all cases, yielding $T_w/T_0 \approx 0.14$ (compared with $T_w/T_0 \approx 0.09$ for the Mach 8 flat plate at altitude), and $R_f = 1.1$. First, the local heat transfer rate at 1.0 m from the leading edge of the Mach 8 flat plate at 35 km from the CFD is 37.3 kW m^{-2}. The local heat transfer rates at the same location from the Mach 5 and 6 vitiated flat plate CFD are factors of 3.4 and 1.3 larger respectively. Therefore, sufficiently far from the leading edge, the local heat transfer rate expected from the Mach 6 vitiated air turbulent flat plate boundary layer case should be about 30% larger than the Mach 8 flat plate at altitude.

Next, comparing the correlation results in figures 16 and 17 with the CFD shows that, as might be expected on cold walls, the van Driest (1956) and Eckert (1955) results tend to over-predict the heat transfer rates. In figure 16, the van Driest (1956) correlation results for the Mach 5 and 6 vitiated air flat plates and Mach 8 flat plate at 1.0 m from the leading edge are 22%, 33% and 40% larger than the CFD results respectively. In figure 17, the Eckert (1955) correlation results are similarly 25%, 32% and 33% larger respectively. In contrast, the Spalding & Chi (1964) results shown in figure 18 agree almost perfectly with the Mach 6 vitiated and Mach 8 flat plate CFD beyond about 0.4 m from the leading edge, while the Mach 5 vitiated flat plate CFD is only under-estimated by about 8% at 1.0 m from the leading edge.

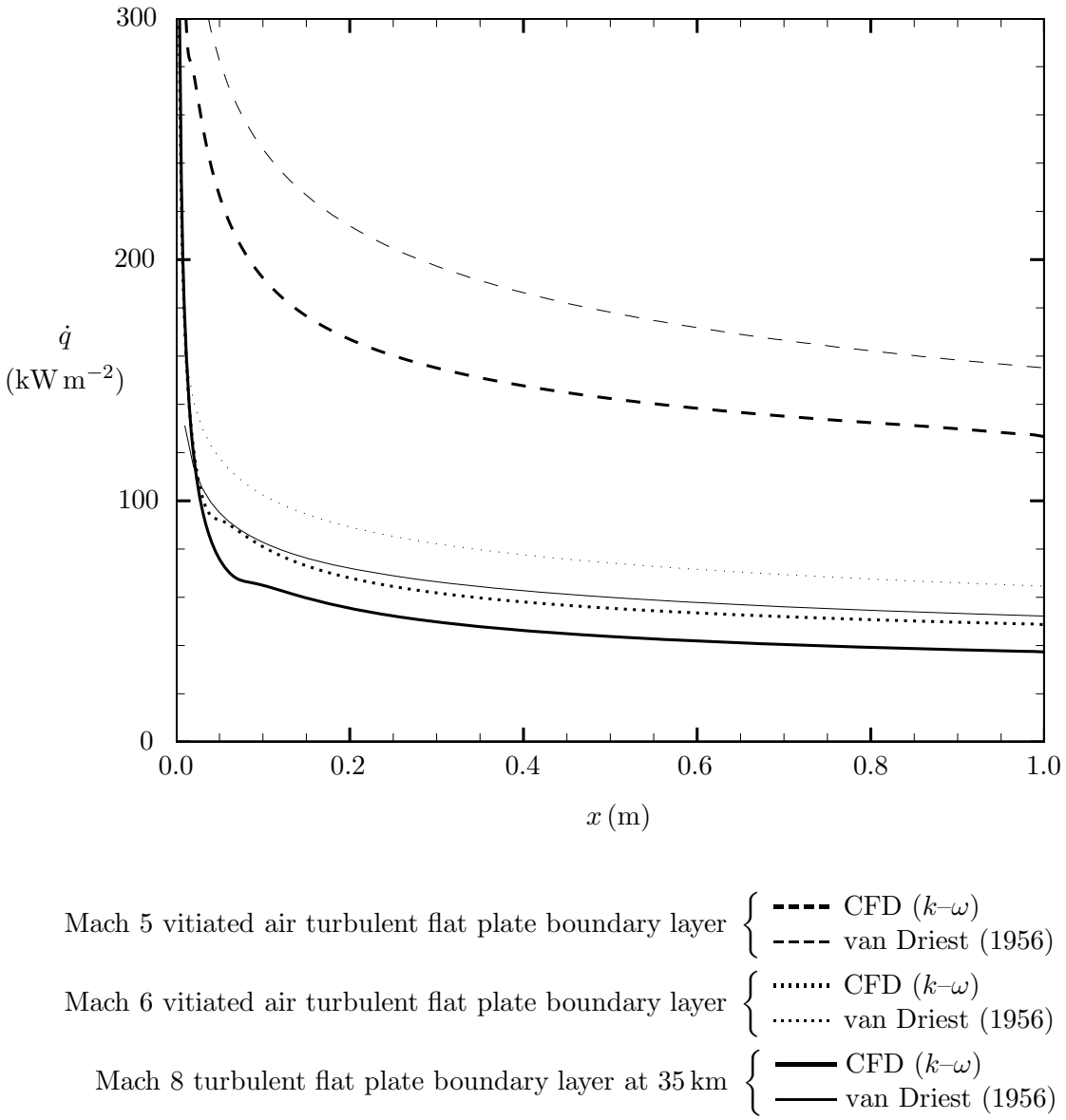

Figure 16: Local heat transfer rates for vitiated air turbulent flat plate boundary layers compared with a Mach 8 flat plate at an altitude of 35 km: van Driest (1956) correlation.

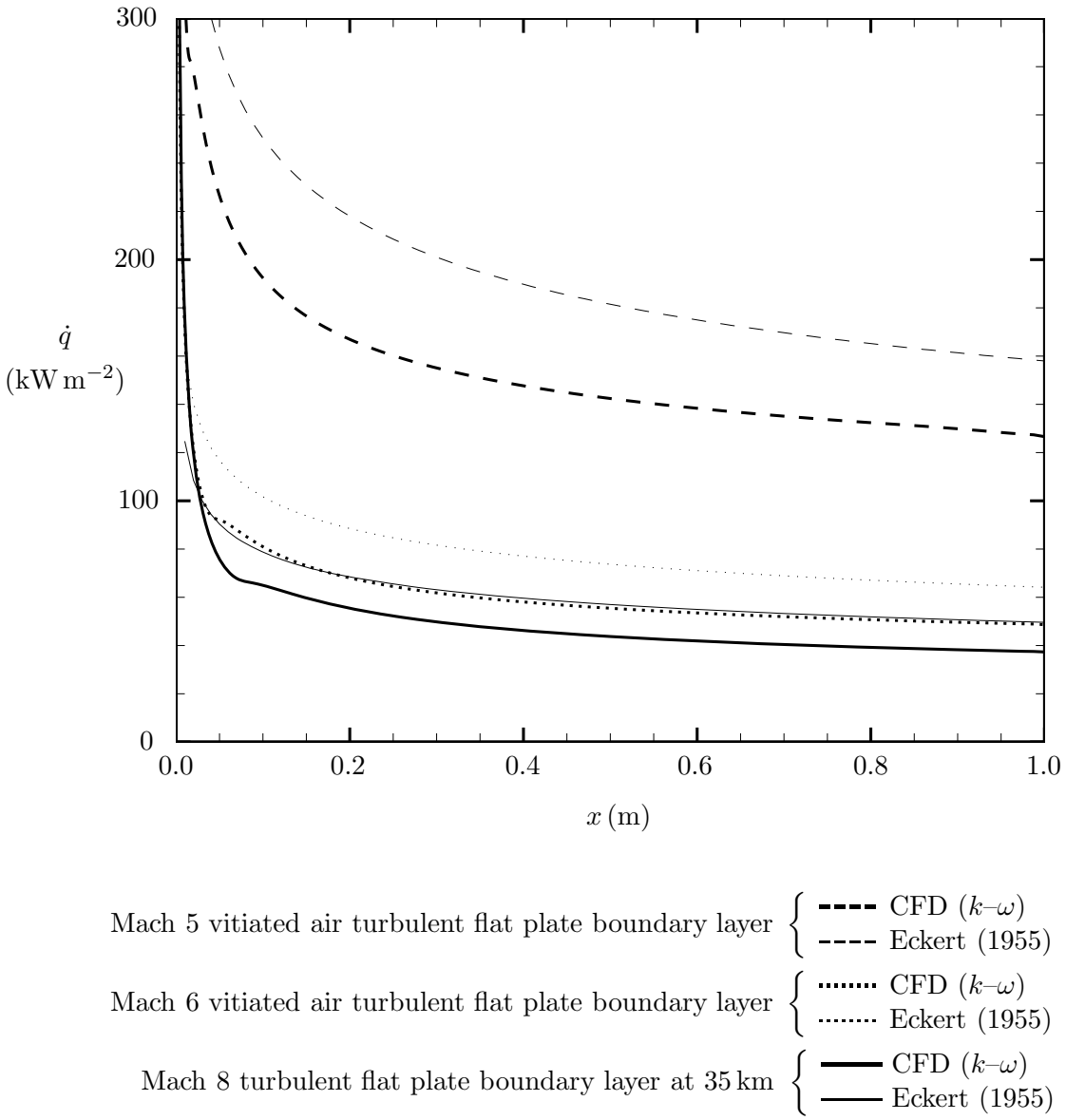

Figure 17: Local heat transfer rates for vitiated air turbulent flat plate boundary layers compared with a Mach 8 flat plate at an altitude of 35 km: Eckert (1955) correlation.

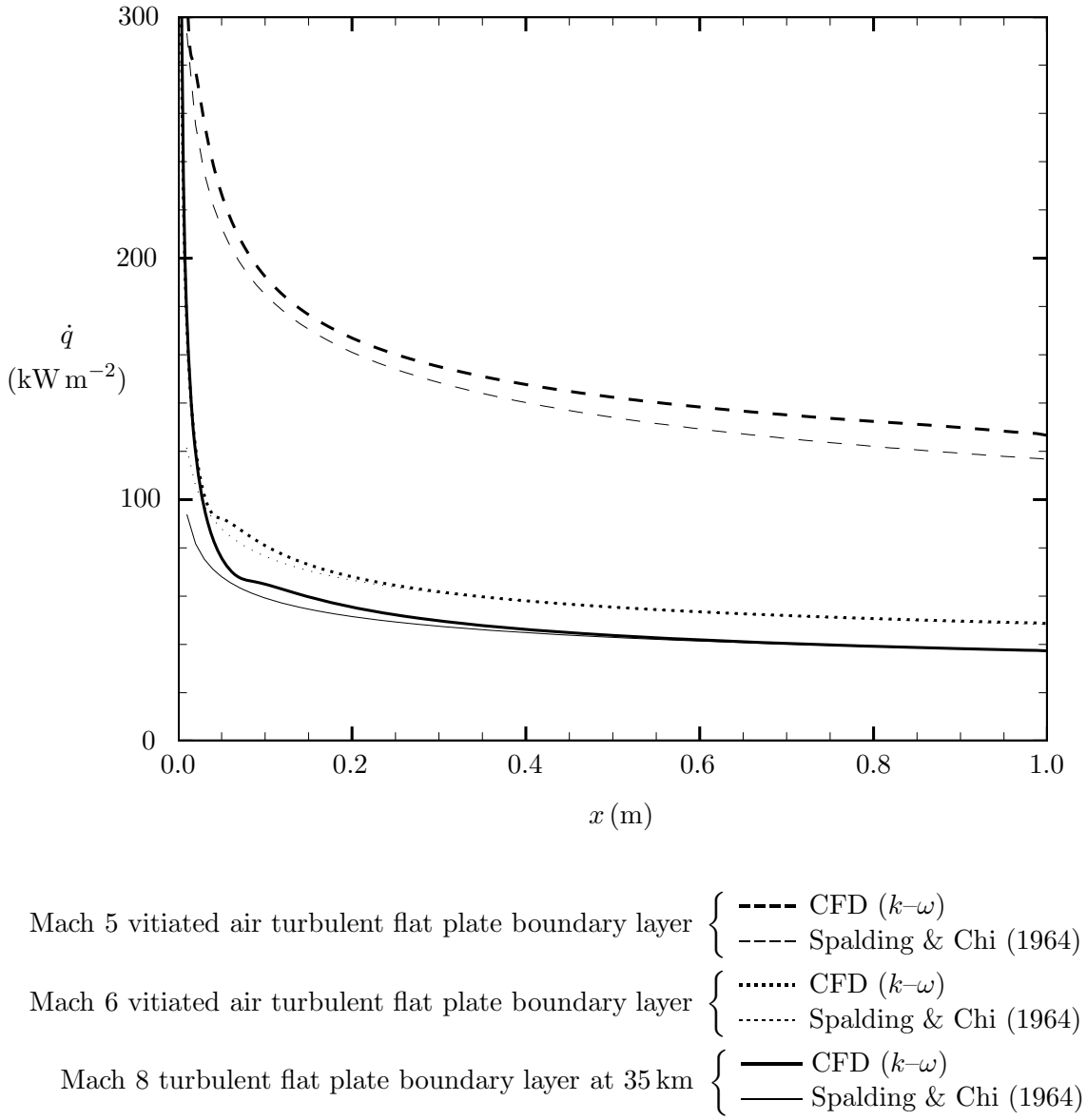

Figure 18: Local heat transfer rates for vitiated air turbulent flat plate boundary layers compared with a Mach 8 flat plate at an altitude of 35 km: Spalding & Chi (1964) correlation.

5 Conclusions

DSTO's participation in the HIFiRE hypersonic vehicle flight test program has renewed interest in aerodynamic heating in high-speed flows. The surface temperatures and heat transfer rates experienced by such vehicles in flight are key pieces of information needed during their design. For simple geometries, these may be estimated very quickly using empirical methods. More detailed analysis of both simple and complicated geometries requires the use of computational fluid dynamics (CFD). Although CFD offers some advantages, it is, by comparison with empirical methods, more difficult to implement and produces results less rapidly.

It is anticipated that empirical methods (referred to herein as 'engineering correlations') will be used in the early stages of hypersonic vehicle design in the HIFiRE Program. This technical report summarizes the results of an investigation into the details and performance of the van Driest (1956), Eckert (1955) and Spalding & Chi (1964) engineering correlation methods for predicting skin friction and heat transfer rates in high-speed flows. These correlations, in the form presented herein, can only be used in zero-pressure-gradient flows. The scope of this report was therefore limited to flow past flat plates, and also wedges and cones with attached shock waves. The author implemented the engineering correlation methods for these geometries in a Fortran 90 code called `zpg_qdot` for a mixture of calorifically imperfect species and arbitrary reference conditions. Both laminar and turbulent compressible boundary layers were considered, but transition was not modelled.

The main result of this report is a series of comparisons with experimental and CFD data of Stanton Numbers, heat transfer rates, skin friction coefficients and viscous length scales computed with the engineering correlations implemented in `zpg_qdot`. The first of these was a comparison with Stanton Numbers measured in hypersonic high-enthalpy laminar, transitional and turbulent flat plate boundary layers in a shock tunnel reported by Goyne, Stalker & Paull (2003). For comparison, laminar and turbulent Stanton Numbers were computed with `zpg_qdot` for stagnation enthalpies of 3.5, 6.5 and 9.0 MJkg^{-1} respectively with a wall temperature of 300 K. Laminar and turbulent CFD was also carried out using a finite-volume structured mesh Navier–Stokes code based on the method of White & Morrison (1999). The laminar Eckert (1955) correlation and laminar CFD curves matched very closely in all cases, and reasonable agreement with the experimental data was also obtained. For the turbulent correlations, van Driest (1956) and Eckert (1955) predicted similar Stanton Numbers that somewhat over-estimated the cluster of experimental measurements. Conversely, the Spalding & Chi (1964) correlation somewhat under-estimated the experimental data. The turbulent CFD results, using the k–ω and Menter-SST turbulence models, fell between the upper and lower estimates of the correlations, and showed good agreement with the turbulent experimental data. In each case, the Menter-SST model predicted a slightly larger Stanton Number than the k–ω model.

These observations raised the following important point. In the absence of a transition model, the turbulent correlation and CFD results would be expected to under-predict the experimental data. It was therefore surprising that either slight over-estimation or reasonable agreement was observed. One reason could be that the Stanton Number data was plotted on logarithmic scales. The effects of the exact location of transition then diminish at large distances from the leading edge of a plate, and Stanton Number profiles

with and without transition may look similar at these locations. It was also concluded that the van Driest (1956) and Eckert (1955) correlations tend to over-predict skin friction and heat transfer rates on cold walls (presently $T_w/T_0 < 0.1$ in all cases), thereby further compensating for the absence of a transition model. Additionally, some doubt existed in the Goyne *et al.* (2003) experiment about the extent to which their boundary layers had relaxed from a transitional to fully turbulent state. Some suppression of the Stanton Numbers measured in their experiment below fully turbulent values might then be expected. This further helps to explain the good agreement between the CFD and experimental data in the absence of a transition model.

The second case considered was a comparison with experimental measurements of Stanton Numbers on a 5° semi-angle cone at a free-stream Mach Number of 7.9 reported by Chien (1974). Cooling was used to control the wall temperature in the experiment, and measurements were made for $T_w/T_0 = 0.35$, 0.20 and 0.11 up to a maximum $Re_x = 21.7 \times 10^6$. For the case $T_w/T_0 = 0.35$, the laminar CFD results agreed very well with the experimental data, but the laminar Eckert (1955) correlation somewhat under-predicted. There was reasonable agreement among the turbulent engineering correlation and CFD results, but these all lay below the cluster of turbulent experimental data points. The turbulent Eckert (1955) and Spalding & Chi (1964) correlations predicted similar Stanton Numbers, and these were found to be somewhat smaller than the van Driest (1956) estimate. For the colder-wall cases with $T_w/T_0 = 0.20$ and 0.11, the laminar CFD and laminar Eckert (1955) correlation results changed very little, and they also showed about the same level of agreement with the experimental data. However, Stanton Numbers from the turbulent CFD results steadily increased as the wall temperature fell, yielding quite reasonable agreement with the turbulent experimental data. The correlation results also changed with decreasing wall temperature. For $T_w/T_0 = 0.11$, the Eckert (1955) and van Driest (1956) curves predicted similar Stanton Numbers that showed close agreement with the experimental data. This result was expected, since the van Driest (1956) and Eckert (1955) correlations are known to over-predict heat transfer on cold walls.

The remaining cases involved comparison of engineering correlation results with CFD data only. The first of these was a comparison of local skin friction coefficients, viscous length scales and heat transfer rates from a Mach 8 flat plate and 10° semi-angle wedge and cone at an altitude of 35 km with $T_w = 300$ K. These scenarios were chosen for investigation because they provide useful information at a Mach Number and altitude that might be encountered in HIFiRE flight tests. For the flat plate, the laminar CFD and laminar Eckert (1955) results overlapped almost exactly in all cases. In the turbulent case, the CFD results agreed most closely with the Spalding & Chi (1964) correlation. The van Driest (1956) and Eckert (1955) correlations over-estimated the CFD by about 30% for the local skin friction coefficient and heat transfer rate, and somewhat underestimated the CFD for the viscous length scale. Of the two turbulence models tested, the Menter-SST model predicted a slightly larger local skin friction coefficient and heat transfer rate and a slightly smaller viscous length scale. Total heat transfer rates at 1.0 m from the leading edge of flat plates at an altitude of 35 km with Mach Numbers in the range 5–10 were also computed. This showed that the Eckert (1955) correlation provided the closest estimate to the CFD results of the total heat transfer rate for both laminar and turbulent boundary layers.

Local heat transfer rates computed for the Mach 8 10° semi-angle wedge were similar

to the Mach 8 flat plate results, but were a factor of 3.5 larger. For the Mach 8 10° semi-angle cone, the local heat transfer rates predicted by the correlations were slightly smaller than those for the wedge. The shape of the cone CFD curve was also somewhat different to the wedge curve, where, compared with the correlations, the cone CFD over-estimated the local heat transfer rate close to the leading edge. Small oscillations also appeared in the cone CFD curve. These numerical artifacts could have stemmed from the stronger interaction between the boundary layer and attached shock-wave in the cone CFD owing to the smaller cone shock-wave angle. Alternatively, they could be caused by the use of cold walls.

In the final case examined, turbulent local heat transfer rates for Mach 5 and 6 flat plates with $T_w = 300\,\mathrm{K}$ immersed in vitiated air were compared with results from the Mach 8 flat plate at 35 km. The use of vitiated air is one way to replicate the large stagnation temperature and enthalpy conditions of hypersonic flight in continuous-flow wind tunnels. The construction of such a facility at DSTO-Melbourne has been proposed, and it is important to understand how the vitiation might affect the local heat transfer rates to flat plates in the wind-tunnel compared with hypersonic flat plates at altitude. CFD results showed that the local heat transfer rate at 1.0 m from the leading edge of the Mach 5 and 6 vitiated air flat plates were factors of 3.4 and 1.3 larger than at the same point on the Mach 8 flat plate. Therefore, the local heat transfer rate expected in the Mach 6 vitiated air flat plate case would be 30% larger than that experienced by a Mach 8 flat plate at altitude. The van Driest (1956) and Eckert (1955) correlations tended to over-estimate the CFD by 20%–40%, but the Spalding & Chi (1964) results agreed very well with the CFD beyond about 0.4 m from the leading edge. These results show that the heat transfer rates experienced by a Mach 8 flat plate at altitude can be achieved in the proposed DSTO-Melbourne facility.

Overall, this investigation showed that engineering correlation methods for predicting heat transfer in zero-pressure-gradient boundary layers can produce results that agree reasonably well with CFD and experimental data. Both laminar and turbulent correlations were considered, but transition was not modelled. Therefore, caution would be required when using the correlations near a point of boundary layer transition. More accurate prediction of heat transfer rates near such a location would require the use of a transition model. Nevertheless, the important conclusion is that the correlations can be used with reasonable confidence for predicting heat transfer rates in hypersonic flows over simple shapes like flat plates, wedges and cones. Parts of the hypersonic vehicles in the HIFiRE Program will be assembled from these types of shapes, so engineering correlation methods therefore have the potential to be an important design tool.

References

Anderson, J. D. 1989 *Hypersonic and High Temperature Gas Dynamics*. McGraw-Hill.

Bertin, J. J. 1994 *Hypersonic Aerothermodynamics*. AIAA.

Bradshaw, P. 1977 Compressible turbulent shear layers. *Ann. Rev. Fluid Mech.* **9**, 33–54.

Brown, P. N., Byrne, G. D. & Hindmarsh, A. C. 1989 VODE: A variable coefficient ODE solver. *SIAM J. Sci. Stat. Comput.* **10**, 1038–1051.

Cary, A. M. 1970 Summary of available information on Reynolds analogy for zero-pressure-gradient, compressible turbulent-boundary-layer flow. *Tech. Rep.* D-5560. NASA Tech. Note.

Chien, K. Y. 1974 Hypersonic turbulent skin-friction and heat-transfer measurements on a sharp cone. *AIAA J.* **12**, 1522–1526.

van Driest, E. R. 1956 The problem of aerodynamic heating. *Aeronaut. Engng Rev.* **15**, 26–41.

Eckert, E. R. G. 1955 Engineering relations for friction and heat transfer to surfaces in high velocity flow. *J. Aeronaut. Sci.* **22**, 585–587.

Goyne, C. P., Stalker, R. J. & Paull, A. 2003 Skin-friction measurements in high-enthalpy hypersonic boundary layers. *J. Fluid Mech.* **485**, 1–32.

Holden, M. S. 1972 An experimental investigation of turbulent boundary layers at high Mach numbers and Reynolds numbers. *Tech. Rep.* CR-112147. NASA Contractor Report.

Hopkins, E. J. & Inouye, M. 1971 An evaluation of theories for predicting turbulent skin friction and heat transfer on flat plates at supersonic and hypersonic Mach numbers. *AIAA J.* **9**, 993–1003.

Kee, R. J., Miller, J. A. & Jefferson, T. H. 1980 CHEMKIN: A General-Purpose Problem-Independent Transportable Fortran Chemical Kinetics Code Package. *Tech. Rep.* SAND80-8003. Sandia National Laboratories Report.

NACA, Ames Research Staff 1953 Equations, tables, and charts for compressible flow. *Tech. Rep.* TR-1135. NACA Tech. Report.

Sims, J. L. 1964 Tables for supersonic flow around right circular cones at zero angle of attack. *Tech. Rep.* SP-3004. NASA Special Publication.

Spalding, D. B. & Chi, S. W. 1964 The drag of a compressible turbulent boundary layer on a smooth flat plate with and without heat transfer. *J. Fluid Mech.* **18**, 117–143.

White, F. M. 1974 *Viscous Fluid Flow*. McGraw-Hill.

White, J. A. & Morrison, J. H. 1999 A pseudo-temporal multigrid relaxation scheme for solving the parabolized Navier–Stokes equations. *AIAA 99-3360* .

Appendix A Goyne *et al.* (2003) high-enthalpy hypersonic boundary layers

Figures A1–A6 summarize the `zpg_qdot` input files `1ns` and `1ns_zpg` and output file `zpgout.txt` used to compute boundary layer properties at $x = 1.5\,\mathrm{m}$ from the leading edge of each Goyne *et al.* (2003) flat plate case listed in table 3. This information was used to determine the wall-normal and stream-wise grid spacing for the corresponding CFD calculations (see discussion to follow). The actual Stanton Number curves computed using `zpg_qdot` shown in figures 7–9 were obtained using the following three additional inputs in the file `1ns_zpg`:

```
  umin = 5.0
  umax = 8.0
divdec = 10
```

Stanton Numbers were therefore computed for Reynolds Numbers Re_x based on the distance from the leading edge in the range 10^5–10^8, with 10 divisions per decade of Re_x.

Table A1 summarizes the local viscous length scales obtained at $x = 1.5\,\mathrm{m}$ from the output file `zpgout.txt` shown in figures A1–A6. The laminar reference temperature viscous length scale is used for the laminar and transitional cases A, B and C. The turbulent reference temperature viscous length scale is used for the transitional and turbulent cases DHKQ, FILR and GJM. The following rules were then used to determine the wall-normal and stream-wise grid spacing used in the CFD calculations. First, the smallest local viscous length scale was rounded-off in both the laminar and turbulent cases. This gives roughly $2 \times 10^{-5}\,\mathrm{m}$ and $2.5 \times 10^{-6}\,\mathrm{m}$ for the laminar and turbulent cases respectively. These are now assumed to be the wall-normal grid spacing at the end ($x = 1.5\,\mathrm{m}$) of the plate, so that $y^+ = O(1)$ there. Next, the wall-normal grid spacing at the leading edge of the plate is assumed to be five times smaller than at the trailing edge. Finally, the stream-wise grid spacing at the leading edge is assumed to be ten times larger than the wall-normal spacing at the leading edge. The remaining grid spacings were set to Gridgen defaults. Table A2 summarizes the two grids, `goyne_lam.grd` and `goyne_tur.grd` for the laminar and turbulent cases respectively, that were generated using these rules.

Condition	$\delta_\nu(x = 1.5\,\mathrm{m})$ (m)
A	4.7×10^{-5}
B	3.6×10^{-5}
C	1.7×10^{-5}
DHKQ	3.5×10^{-6}
FILR	2.5×10^{-6}
GJM	2.4×10^{-6}

Table A1: Local viscous length scales computed with the Eckert (1955) reference temperature method at $x = 1.5\,\mathrm{m}$ from the leading edge of each Goyne *et al.* (2003) flat plate case listed in table 3.

```
>---

>TXT
       ***** goyne_A flat plate *****
>END

>PRM
     &CMEX_PARAMETERS initial_pressure = 870.0,
                      initial_mach_number = 6.4,
                      default_initial_temperature = 486.0 /

     >SPC
         2
         N2  0.77
         O2  0.23
     >END

     >RUN
        1
        ISEN 1.0e0
     >END

     >RCT
        &REAC_PARAMETERS /
     >END

     >VOD
        &VODE_PARAMETERS /
     >END

>END

>---
```

(a) `1ns`

```
&ZPG_QDOT_PARAMETERS           T_wall = 300.0,
                           platelength = 1.5,
                               xpoints = 100,
                             shockcase = 0,
                         RefTempMethod = 1,
                               prandtl = 0.72,
                 Reynolds_analogy_factor = 1.0 /
```

(b) `1ns_zpg`

```
                    * * * FLAT PLATE * * *

Mach Num.   Re/x[1/m]   D[kg/m^3]    StatT[K] LAdWallT[K] TAdWallT[K]

    6.400   6.575E+05   6.210E-03       486.0      3239.1      3383.6


                    Local cf, delta_nu = nu_wall/u_tau and q_dot
                    --------------------------------------------

                                                  RefTempMethod
                                                 1. Eckert (1955)

          x =  1.500  Van Driest    Spalding   Lam Ref.T   Tur Ref.T

        T_wall [K]       300.0       300.0       300.0       300.0

               F_c       1.689       1.689       2.055       2.120
           F_Rex         0.852       5.392       0.279       0.263
           Rex_i     8.404E+05   5.317E+06   2.753E+05   2.597E+05
          T* [K]         ---         ---       998.678    1030.474

              cf     2.290E-03   1.583E-03   6.158E-04   2.307E-03

      delta_nu [m]   2.454E-05   2.951E-05   4.731E-05   2.444E-05

      qdot [W/m^2]   7.531E+04   5.207E+04   2.394E+04   7.588E+04


                    Total heat transfer rate per unit plate width
                    ---------------------------------------------

          x =  1.500  Van Driest    Spalding   Lam Ref.T   Tur Ref.T

        Qdot [W/m]   1.412E+05   9.764E+04   5.770E+04   1.423E+05


                    Radiation and wall heat transfer rates: Case 0
                    ----------------------------------------------

                    User input: wall temperature [K] =  300.0

          x =  1.500  Van Driest    Spalding   Lam Ref.T   Tur Ref.T

      qr_dot [W/m]   0.000E+00   0.000E+00   0.000E+00   0.000E+00

      qs_dot [W/m]   7.531E+04   5.207E+04   2.394E+04   7.588E+04
```

(c) `zpgout.txt`

Figure A1: `zpg_qdot` file input-output for Goyne *et al.* (2003) case A. (a) `cmpexp` input. (b) `zpgqdot` input. (c) `zpgqdot` output.

```
>---

>TXT
       ***** goyne_B flat plate *****
>END

>PRM
     &CMEX_PARAMETERS initial_pressure = 1030.0,
                      initial_mach_number = 6.2,
                      default_initial_temperature = 772.0 /

     >SPC
         2
         N2  0.77
         O2  0.23
     >END

     >RUN
        1
        ISEN 1.0e0
     >END

     >RCT
        &REAC_PARAMETERS /
     >END

     >VOD
        &VODE_PARAMETERS /
     >END

>END

>---
```

(a) `1ns`

```
&ZPG_QDOT_PARAMETERS           T_wall = 300.0,
                           platelength = 1.5,
                               xpoints = 100,
                             shockcase = 0,
                         RefTempMethod = 1,
                               prandtl = 0.72,
                 Reynolds_analogy_factor = 1.0 /
```

(b) `1ns_zpg`

```
                    * * * FLAT PLATE * * *

Mach Num.   Re/x[1/m]   D[kg/m^3]    StatT[K] LAdWallT[K] TAdWallT[K]

    6.200   4.187E+05   4.628E-03       772.0      4629.5      4835.3


                        Local cf, delta_nu = nu_wall/u_tau and q_dot
                        --------------------------------------------

                                                    RefTempMethod
                                                   1. Eckert (1955)

          x =  1.500  Van Driest    Spalding   Lam Ref.T   Tur Ref.T

        T_wall [K]       300.0       300.0       300.0       300.0

               F_c       1.443       1.443       1.794       1.852
           F_Rex         1.410      11.508       0.334       0.314
           Rex_i     8.852E+05   7.227E+06   2.099E+05   1.969E+05
          T* [K]       ---         ---        1384.647    1429.917

              cf     2.653E-03   1.743E-03   8.081E-04   2.791E-03

      delta_nu [m]   2.010E-05   2.480E-05   3.642E-05   1.960E-05

      qdot [W/m^2]   1.190E+05   7.817E+04   4.292E+04   1.252E+05


                        Total heat transfer rate per unit plate width
                        ---------------------------------------------

          x =  1.500  Van Driest    Spalding   Lam Ref.T   Tur Ref.T

        Qdot [W/m]     2.230E+05   1.466E+05   1.034E+05   2.347E+05


                       Radiation and wall heat transfer rates: Case 0
                       ----------------------------------------------

                       User input: wall temperature [K] =  300.0

          x =  1.500  Van Driest    Spalding   Lam Ref.T   Tur Ref.T

      qr_dot [W/m]     0.000E+00   0.000E+00   0.000E+00   0.000E+00

      qs_dot [W/m]     1.190E+05   7.817E+04   4.292E+04   1.252E+05
```

(c) `zpgout.txt`

Figure A2: `zpg_qdot` file input-output for Goyne *et al.* (2003) case B. (a) `cmpexp` input. (b) `zpgqdot` input. (c) `zpgqdot` output.

```
>---

>TXT
       ***** goyne_C flat plate *****
>END

>PRM
     &CMEX_PARAMETERS initial_pressure = 2700.0,
                      initial_mach_number = 5.9,
                      default_initial_temperature = 1010.0 /

     >SPC
         2
         N2  0.77
         O2  0.23
     >END

     >RUN
        1
        ISEN 1.0e0
     >END

     >RCT
        &REAC_PARAMETERS /
     >END

     >VOD
        &VODE_PARAMETERS /
     >END

>END

>---
```

(a) `1ns`

```
&ZPG_QDOT_PARAMETERS           T_wall = 300.0,
                           platelength = 1.5,
                               xpoints = 100,
                             shockcase = 0,
                          RefTempMethod = 1,
                               prandtl = 0.72,
                 Reynolds_analogy_factor = 1.0 /
```

(b) `1ns_zpg`

```
                    * * * FLAT PLATE * * *

Mach Num.   Re/x[1/m]   D[kg/m^3]    StatT[K] LAdWallT[K] TAdWallT[K]

    5.900   7.271E+05   9.273E-03      1010.0      5000.0      5000.0


                        Local cf, delta_nu = nu_wall/u_tau and q_dot
                        --------------------------------------------

                                                  RefTempMethod
                                                 1. Eckert (1955)

          x =  1.500  Van Driest    Spalding   Lam Ref.T   Tur Ref.T

        T_wall [K]       300.0       300.0       300.0       300.0

               F_c       1.193       1.193       1.518       1.518
           F_Rex         2.125      17.254       0.445       0.445
           Rex_i     2.317E+06   1.882E+07   4.855E+05   4.855E+05
          T* [K]           ---         ---    1532.800    1532.800

              cf     2.648E-03   1.742E-03   6.279E-04   2.844E-03

       delta_nu [m]   8.130E-06   1.002E-05   1.670E-05   7.845E-06

       qdot [W/m^2]   3.080E+05   2.026E+05   8.662E+04   3.308E+05


                        Total heat transfer rate per unit plate width
                        ---------------------------------------------

          x =  1.500  Van Driest    Spalding   Lam Ref.T   Tur Ref.T

        Qdot [W/m]     5.774E+05   3.798E+05   2.087E+05   6.202E+05


                       Radiation and wall heat transfer rates: Case 0
                       ----------------------------------------------

                       User input: wall temperature [K] =  300.0

          x =  1.500  Van Driest    Spalding   Lam Ref.T   Tur Ref.T

       qr_dot [W/m]    0.000E+00   0.000E+00   0.000E+00   0.000E+00

       qs_dot [W/m]    3.080E+05   2.026E+05   8.662E+04   3.308E+05
```

(c) `zpgout.txt`

Figure A3: `zpg_qdot` file input-output for Goyne *et al.* (2003) case C. (a) `cmpexp` input. (b) `zpgqdot` input. (c) `zpgqdot` output.

```
>---

>TXT
      ***** goyne_DHKQ flat plate *****
>END

>PRM
     &CMEX_PARAMETERS initial_pressure = 8140.0,
                      initial_mach_number = 6.6,
                      default_initial_temperature = 336.0 /

     >SPC
         2
         N2  0.77
         O2  0.23
     >END

     >RUN
        1
        ISEN 1.0e0
     >END

     >RCT
        &REAC_PARAMETERS /
     >END

     >VOD
        &VODE_PARAMETERS /
     >END

>END

>---
```

(a) `1ns`

```
&ZPG_QDOT_PARAMETERS           T_wall = 300.0,
                           platelength = 1.5,
                               xpoints = 100,
                             shockcase = 0,
                         RefTempMethod = 1,
                               prandtl = 0.72,
                 Reynolds_analogy_factor = 1.0 /
```

(b) `1ns_zpg`

```
                    * * * FLAT PLATE * * *

Mach Num.   Re/x[1/m]   D[kg/m^3]    StatT[K] LAdWallT[K] TAdWallT[K]

    6.600   1.010E+07   8.404E-02       336.0      2448.8      2558.1

                        Local cf, delta_nu = nu_wall/u_tau and q_dot
                        --------------------------------------------

                                                RefTempMethod
                                               1. Eckert (1955)

          x =  1.500  Van Driest    Spalding   Lam Ref.T   Tur Ref.T

          T_wall [K]       300.0       300.0       300.0       300.0

                 F_c       1.940       1.940       2.330       2.401
               F_Rex       0.563       2.920       0.228       0.216
               Rex_i    8.527E+06   4.426E+07   3.452E+06   3.271E+06
              T* [K]         ---         ---       782.826     806.861

                  cf   1.254E-03   9.025E-04   1.534E-04   1.227E-03

        delta_nu [m]   3.422E-06   4.035E-06   9.787E-06   3.460E-06

        qdot [W/m^2]   3.429E+05   2.467E+05   4.944E+04   3.354E+05


                        Total heat transfer rate per unit plate width
                        ---------------------------------------------

          x =  1.500  Van Driest    Spalding   Lam Ref.T   Tur Ref.T

          Qdot [W/m]   6.429E+05   4.625E+05   1.192E+05   6.289E+05


                       Radiation and wall heat transfer rates: Case 0
                       ----------------------------------------------

                       User input: wall temperature [K] =  300.0

          x =  1.500  Van Driest    Spalding   Lam Ref.T   Tur Ref.T

        qr_dot [W/m]   0.000E+00   0.000E+00   0.000E+00   0.000E+00

        qs_dot [W/m]   3.429E+05   2.467E+05   4.944E+04   3.354E+05
```

(c) `zpgout.txt`

Figure A4: `zpg_qdot` file input-output for Goyne *et al.* (2003) cases DHKQ. (a) `cmpexp` input. (b) `zpgqdot` input. (c) `zpgqdot` output.

```
>---

>TXT
      ***** goyne_FILR flat plate *****
>END

>PRM
     &CMEX_PARAMETERS initial_pressure = 10880.0,
                      initial_mach_number = 6.0,
                      default_initial_temperature = 741.0 /

     >SPC
         2
         N2  0.77
         O2  0.23
     >END

     >RUN
        1
        ISEN 1.0e0
     >END

     >RCT
        &REAC_PARAMETERS /
     >END

     >VOD
        &VODE_PARAMETERS /
     >END

>END

>---
```

(a) `1ns`

```
 &ZPG_QDOT_PARAMETERS           T_wall = 300.0,
                            platelength = 1.5,
                                xpoints = 100,
                              shockcase = 0,
                           RefTempMethod = 1,
                                 prandtl = 0.72,
                 Reynolds_analogy_factor = 1.0 /
```

(b) `1ns_zpg`

```
                        * * * FLAT PLATE * * *


Mach Num.    Re/x[1/m]   D[kg/m^3]    StatT[K] LAdWallT[K] TAdWallT[K]

    6.000   4.514E+06   5.093E-02       741.0      4241.3      4427.7


                        Local cf, delta_nu = nu_wall/u_tau and q_dot
                        --------------------------------------------

                                                  RefTempMethod
                                                 1. Eckert (1955)

          x =  1.500  Van Driest    Spalding   Lam Ref.T   Tur Ref.T

          T_wall [K]       300.0       300.0       300.0       300.0

                 F_c       1.414       1.414       1.742       1.797
               F_Rex       1.394      10.659       0.357       0.336
               Rex_i   9.436E+06   7.218E+07   2.417E+06   2.273E+06
              T* [K]         ---         ---    1290.575    1331.581

                  cf   1.686E-03   1.122E-03   2.452E-04   1.764E-03

         delta_nu [m]   2.463E-06   3.019E-06   6.460E-06   2.409E-06

         qdot [W/m^2]   7.139E+05   4.752E+05   1.230E+05   7.468E+05


                        Total heat transfer rate per unit plate width
                        ---------------------------------------------

          x =  1.500  Van Driest    Spalding   Lam Ref.T   Tur Ref.T

          Qdot [W/m]   1.339E+06   8.911E+05   2.964E+05   1.400E+06


                       Radiation and wall heat transfer rates: Case 0
                       ----------------------------------------------

                       User input: wall temperature [K] =  300.0

          x =  1.500  Van Driest    Spalding   Lam Ref.T   Tur Ref.T

         qr_dot [W/m]   0.000E+00   0.000E+00   0.000E+00   0.000E+00

         qs_dot [W/m]   7.139E+05   4.752E+05   1.230E+05   7.468E+05
```

(c) `zpgout.txt`

Figure A5: `zpg_qdot` file input-output for Goyne *et al.* (2003) cases FILR. (a) `cmpexp` input. (b) `zpgqdot` input. (c) `zpgqdot` output.

```
>---

>TXT
       ***** goyne_GJM flat plate *****
>END

>PRM
     &CMEX_PARAMETERS initial_pressure = 10080.0,
                      initial_mach_number = 5.7,
                      default_initial_temperature = 1147.0 /

     >SPC
         2
         N2  0.77
         O2  0.23
     >END

     >RUN
        1
        ISEN 1.0e0
     >END

     >RCT
        &REAC_PARAMETERS /
     >END

     >VOD
        &VODE_PARAMETERS /
     >END

>END

>---
```

(a) `1ns`

```
&ZPG_QDOT_PARAMETERS           T_wall = 300.0,
                           platelength = 1.5,
                               xpoints = 100,
                             shockcase = 0,
                         RefTempMethod = 1,
                               prandtl = 0.72,
                 Reynolds_analogy_factor = 1.0 /
```

(b) `1ns_zpg`

```
                    * * * FLAT PLATE * * *

Mach Num.   Re/x[1/m]   D[kg/m^3]    StatT[K] LAdWallT[K] TAdWallT[K]

    5.700   2.190E+06   3.048E-02      1147.0      5000.0      5000.0


                        Local cf, delta_nu = nu_wall/u_tau and q_dot
                        --------------------------------------------

                                                  RefTempMethod
                                                 1. Eckert (1955)

          x =  1.500  Van Driest    Spalding   Lam Ref.T   Tur Ref.T

        T_wall [K]       300.0       300.0       300.0       300.0

               F_c       1.081       1.081       1.370       1.370
           F_Rex         2.624      20.803       0.539       0.539
           Rex_i     8.621E+06   6.834E+07   1.771E+06   1.771E+06
          T* [K]       ---         ---        1571.160    1571.160

              cf     2.245E-03   1.484E-03   3.642E-04   2.432E-03

      delta_nu [m]   2.456E-06   3.021E-06   6.097E-06   2.359E-06

      qdot [W/m^2]   9.433E+05   6.235E+05   1.817E+05   1.022E+06


                        Total heat transfer rate per unit plate width
                        ---------------------------------------------

          x =  1.500  Van Driest    Spalding   Lam Ref.T   Tur Ref.T

        Qdot [W/m]     1.769E+06   1.169E+06   4.378E+05   1.916E+06


                       Radiation and wall heat transfer rates: Case 0
                       ----------------------------------------------

                       User input: wall temperature [K] =  300.0

          x =  1.500  Van Driest    Spalding   Lam Ref.T   Tur Ref.T

      qr_dot [W/m]     0.000E+00   0.000E+00   0.000E+00   0.000E+00

      qs_dot [W/m]     9.433E+05   6.235E+05   1.817E+05   1.022E+06
```

(c) `zpgout.txt`

Figure A6: `zpg_qdot` file input-output for Goyne *et al.* (2003) cases GJM. (a) `cmpexp` input. (b) `zpgqdot` input. (c) `zpgqdot` output.

	`goyne_lam.grd`	`goyne_tur.grd`
$x_{\max}$ (m)	1.5	1.5
$y_{\max}$ (m)	0.1	0.1
$i_{\max}$	641	641
$j_{\max}$	97	97
$\Delta_n(i_{\min}, j_{\min})$ (m)	4.0×10^{-6}	4.0×10^{-7}
$\Delta_n(i_{\max}, j_{\min})$ (m)	2.0×10^{-5}	2.0×10^{-6}
$\Delta_n(i_{\text{min–max}}, j_{\max})$ (m)	7.0×10^{-3}	1.0×10^{-2}
$\Delta_s(i_{\min}, j_{\text{min–max}})$ (m)	4.0×10^{-5}	4.0×10^{-6}
$\Delta_s(i_{\max}, j_{\text{min–max}})$ (m)	1.6×10^{-2}	2.2×10^{-2}

Table A2: Grid parameters for the Goyne *et al.* (2003) flat plate cases. Here Δ_s and Δ_n are the stream-wise and wall-normal grid spacings respectively.

Condition	Turbulence Model	Multi-grid cycle	Solution
A	laminar	I	first-order
B	laminar	I	first-order
C	laminar	I	first-order
DHKQ	k–ω, Menter-SST	V	first- and higher-order
FILR	k–ω, Menter-SST	V	first-order
GJM	k–ω, Menter-SST	I	first-order

Table A3: CFD inputs for the Goyne *et al.* (2003) flat plate cases.

Severe convergence difficulties were encountered in most of the Goyne *et al.* (2003) flat-plate CFD cases. It was thought that these problems were caused by the high stagnation enthalpies. The convergence problems were eventually overcome by changing the type of multi-grid cycle and order of the solution. Table A3 summarizes the selection of these schemes for each case. The iteration and CFL scheme was identical in all cases. Here 500 iterations were performed on each of three coarse grid levels, while the CFL number was increased linearly from 0.1 to 3.0 over each level. Iteration proceeded on the finest grid level until six orders of magnitude reduction in the residuals was achieved. The CFL number was increased linearly from 0.1 to 3.0 over the first 1500 iterations on the fine grid, and then was raised to 30.0 over a further 5000 iterations.

Figure A7 shows the sum of the density residuals from the CFD calculations of the Goyne *et al.* (2003) 3.5, 6.5 and 9.0 $\mathrm{MJ\,kg^{-1}}$ laminar and turbulent flat plate boundary layer calculations shown in figures 7–9. It was found that all the laminar cases and the highest-enthalpy turbulent case GJM were the most unstable, and that only first-order solutions could be obtained using multi-grid I cycles. The residuals from these cases converged more slowly compared with the turbulent cases that used multi-grid V cycles.

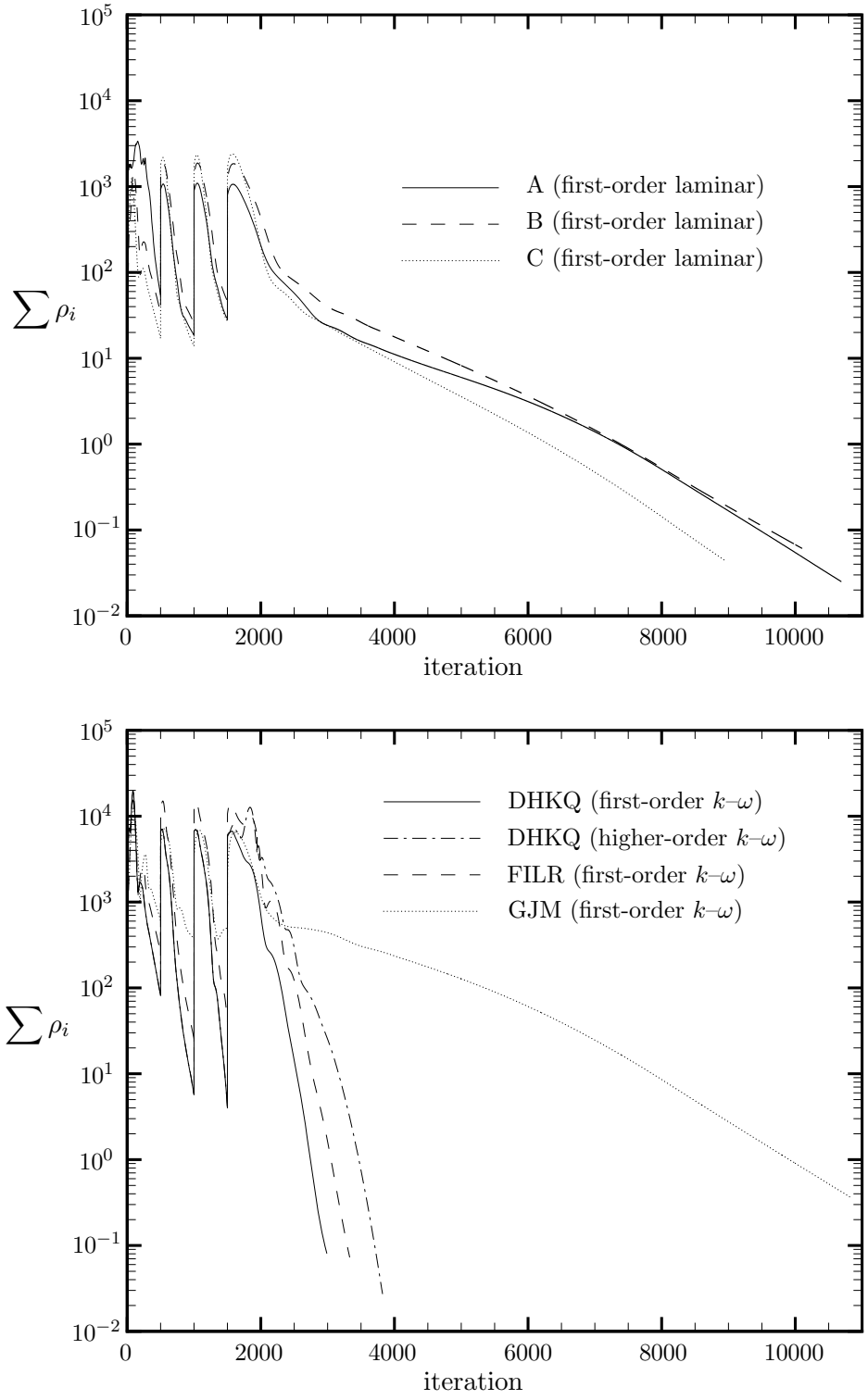

Figure A7: Sum of the density residuals from the CFD calculations of the Goyne *et al.* (2003) 3.5, 6.5 and 9.0 MJ kg^{-1} laminar and turbulent flat plate boundary layer calculations shown in figures 7–9.

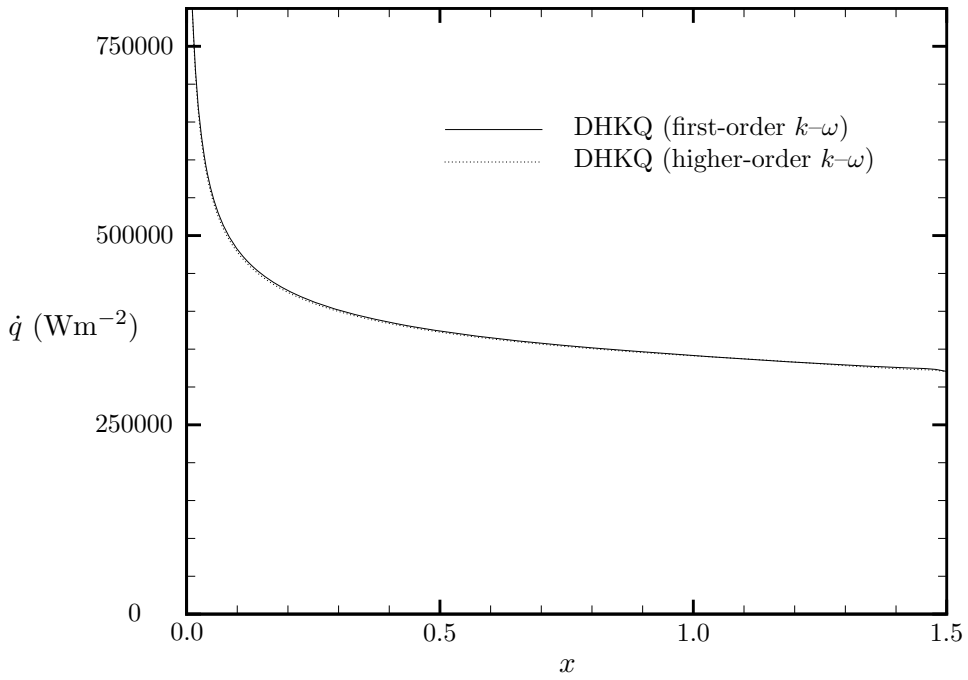

Figure A8: Comparison of the local heat transfer rate from first- and higher-order CFD calculations of the Goyne *et al.* (2003) 3.5 MJ kg^{-1} turbulent flat plate boundary layer case DHKQ.

Both first- and higher-order solutions were able to be obtained for turbulent case DHKQ with the smallest stagnation enthalpy. The resulting residual plots shown in figure A7 are similar in both cases, with the higher-order scheme requiring slightly more iterations to achieve the six-orders of magnitude reduction. Figure A8 shows that there is little difference between the resulting local heat-transfer rates from the first- and higher-order calculations. Although similar comparisons could not be made for the laminar and higher-enthalpy turbulent cases, it would seem reasonable to assume that similarly small differences might be observed.

Appendix B Chien (1974) Mach 7.9 5° semi-angle cone

Figures B1–B3 summarize the `zpg_qdot` input files `1ns` and `1ns_zpg` and output file `zpgout.txt` used to compute boundary layer properties at $x' = 0.6\,\mathrm{m}$ from the leading edge of each Chien (1974) 5° semi-angle cone case listed in table 4. (Here x' is a coordinate parallel to the surface of the cone in a stream-wise plane.) This information was used to determine the wall-normal and stream-wise grid spacing for the corresponding CFD calculations (see discussion to follow).

Table B1 summarizes the local viscous length scales obtained at $x' = 0.6\,\mathrm{m}$ from the output file `zpgout.txt` shown in figures B1–B3. These were obtained with the laminar and turbulent Eckert (1955) reference temperature methods respectively. These length scales were used to determine the wall-normal and stream-wise CFD grid spacings using the rules described in Appendix A. Three grids were then generated, and the details of these are summarized in table B2.

T_w/T_0	$\delta_\nu(x' = 0.6\,\mathrm{m})$ (m)
0.11 (laminar)	4.0×10^{-6}
0.20 (laminar)	8.8×10^{-6}
0.35 (laminar)	2.1×10^{-5}
0.11 (turbulent)	1.8×10^{-6}
0.20 (turbulent)	4.0×10^{-6}
0.35 (turbulent)	1.0×10^{-5}

Table B1: Local viscous length scales computed with the Eckert (1955) reference temperature method at $x' = 0.6\,\mathrm{m}$ from the leading edge of each Chien (1974) 5° semi-angle cone case listed in table 4.

	`chien_0.11.grd`	`chien_0.20.grd`	`chien_0.35.grd`
$x'_{\max}$ (m)	0.6	0.6	0.6
$y'_{\max}$ (m)	0.1	0.1	0.1
$i_{\max}$	641	641	641
$j_{\max}$	97	97	97
$\Delta_n(i_{\min}, j_{\min})$ (m)	2.0×10^{-7}	4.0×10^{-7}	1.0×10^{-6}
$\Delta_n(i_{\max}, j_{\min})$ (m)	1.0×10^{-6}	2.0×10^{-6}	5.0×10^{-6}
$\Delta_n(i_{\text{min–max}}, j_{\max})$ (m)	4.0×10^{-3}	4.0×10^{-3}	4.0×10^{-3}
$\Delta_s(i_{\min}, j_{\text{min–max}})$ (m)	2.0×10^{-6}	4.0×10^{-6}	1.0×10^{-5}
$\Delta_s(i_{\max}, j_{\text{min–max}})$ (m)	4.0×10^{-3}	4.0×10^{-3}	4.0×10^{-3}

Table B2: Grid parameters for the Chien (1974) 5° semi-angle cone cases. Here x' and y' are coordinates parallel and normal to the surface of the cone in a stream-wise plane, and Δ_s and Δ_n are the associated stream-wise and wall-normal grid spacings.

```
>---

>TXT
       ***** Chien 5 degree cone Tw/T0 = 0.11 *****
>END

>PRM
     &CMEX_PARAMETERS initial_pressure = 1.5086e7,
                      initial_mach_number = 0.0,
                      default_initial_temperature = 812.0 /

     >SPC
         2
         N2  0.77
         O2  0.23
     >END

     >RUN
        2
        ISEN 0.000147
        SHCK 1.4168
     >END

     >RCT
        &REAC_PARAMETERS /
     >END

     >VOD
        &VODE_PARAMETERS /
     >END

>END

>---
```

(a) `1ns`

```
   &ZPG_QDOT_PARAMETERS           T_wall = 88.0,
                             platelength = 0.60,
                                 xpoints = 100,
                               shockcase = 2,
                           RefTempMethod = 1,
                                 prandtl = 0.72,
                  Reynolds_analogy_factor = 1.0 /
```

(b) `1ns_zpg`

```
                          * * * CONE * * *

Mach Num.   Re/x[1/m]   D[kg/m^3]    StatT[K] LAdWallT[K] TAdWallT[K]

    7.154   3.448E+07   1.423E-01        75.0       705.8       739.5


                        Local cf, delta_nu = nu_wall/u_tau and q_dot
                        --------------------------------------------

                                                  RefTempMethod
                                                 1. Eckert (1955)

          x =  0.600  Van Driest    Spalding   Lam Ref.T   Tur Ref.T

          T_wall [K]        88.0        88.0        88.0        88.0

                 F_c       2.404       2.404       2.938       3.037
              F_Rex        0.382       1.923       0.148       0.140
              Rex_i    7.895E+06   3.978E+07   3.071E+06   2.893E+06
             T* [K]         ---         ---       220.268     227.682

                 cf    1.209E-03   8.748E-04   2.233E-04   1.169E-03

        delta_nu [m]   1.725E-06   2.028E-06   4.013E-06   1.754E-06

        qdot [W/m^2]   7.183E+04   5.198E+04   1.562E+04   6.948E+04


                        Total heat transfer rate per unit plate width
                        ---------------------------------------------

          x =  0.600  Van Driest    Spalding   Lam Ref.T   Tur Ref.T

          Qdot [W/m]   4.781E+04   3.460E+04   9.674E+03   4.624E+04


                       Radiation and wall heat transfer rates: Case 0
                       ----------------------------------------------

                       User input: wall temperature [K] =   88.0

          x =  0.600  Van Driest    Spalding   Lam Ref.T   Tur Ref.T

        qr_dot [W/m]   0.000E+00   0.000E+00   0.000E+00   0.000E+00

        qs_dot [W/m]   7.183E+04   5.198E+04   1.562E+04   6.948E+04
```

(c) `zpgout.txt`

Figure B1: `zpg_qdot` file input-output for Chien (1974) case $T_w/T_0 = 0.11$. (a) `cmpexp` input. (b) `zpgqdot` input. (c) `zpgqdot` output.

```
>---

>TXT
       ***** Chien 5 degree cone Tw/T0 = 0.20 *****
>END

>PRM
     &CMEX_PARAMETERS initial_pressure = 1.5072e7,
                      initial_mach_number = 0.0,
                      default_initial_temperature = 808.0 /

     >SPC
         2
         N2  0.77
         O2  0.23
     >END

     >RUN
        2
        ISEN 0.000147
        SHCK 1.4168
     >END

     >RCT
        &REAC_PARAMETERS /
     >END

     >VOD
        &VODE_PARAMETERS /
     >END

>END

>---
```

(a) `1ns`

```
   &ZPG_QDOT_PARAMETERS           T_wall = 158.0,
                             platelength = 0.60,
                                 xpoints = 100,
                               shockcase = 2,
                           RefTempMethod = 1,
                                 prandtl = 0.72,
                  Reynolds_analogy_factor = 1.0 /
```

(b) `1ns_zpg`

```
                          * * * CONE * * *

 Mach Num.    Re/x[1/m]   D[kg/m^3]    StatT[K] LAdWallT[K] TAdWallT[K]

     7.154   3.474E+07   1.429E-01        74.6       702.3       735.8


                         Local cf, delta_nu = nu_wall/u_tau and q_dot
                         --------------------------------------------

                                                  RefTempMethod
                                                 1. Eckert (1955)

           x =  0.600  Van Driest    Spalding   Lam Ref.T   Tur Ref.T

          T_wall [K]       158.0       158.0       158.0       158.0

                 F_c       2.855       2.855       3.411       3.510
               F_Rex       0.200       0.678       0.114       0.108
               Rex_i   4.163E+06   1.413E+07   2.377E+06   2.258E+06
              T* [K]         ---         ---     254.381     261.763

                  cf   1.157E-03   9.059E-04   2.187E-04   1.063E-03

         delta_nu [m]   3.804E-06   4.299E-06   8.750E-06   3.968E-06

         qdot [W/m^2]   6.113E+04   4.787E+04   1.351E+04   5.619E+04


                         Total heat transfer rate per unit plate width
                         ---------------------------------------------

           x =  0.600  Van Driest    Spalding   Lam Ref.T   Tur Ref.T

           Qdot [W/m]   4.073E+04   3.190E+04   8.390E+03   3.744E+04


                        Radiation and wall heat transfer rates: Case 0
                        ----------------------------------------------

                        User input: wall temperature [K] =  158.0

           x =  0.600  Van Driest    Spalding   Lam Ref.T   Tur Ref.T

         qr_dot [W/m]   0.000E+00   0.000E+00   0.000E+00   0.000E+00

         qs_dot [W/m]   6.113E+04   4.787E+04   1.351E+04   5.619E+04
```

(c) `zpgout.txt`

Figure B2: `zpg_qdot` file input-output for Chien (1974) case $T_w/T_0 = 0.20$. (a) `cmpexp` input. (b) `zpgqdot` input. (c) `zpgqdot` output.

```
>---

>TXT
       ***** Chien 5 degree cone Tw/T0 = 0.35 *****
>END

>PRM
     &CMEX_PARAMETERS initial_pressure = 1.3128e7,
                      initial_mach_number = 0.0,
                      default_initial_temperature = 814.0 /

     >SPC
         2
         N2  0.77
         O2  0.23
     >END

     >RUN
        2
        ISEN 0.0001505e0
        SHCK 1.4168
     >END

     >RCT
        &REAC_PARAMETERS /
     >END

     >VOD
        &VODE_PARAMETERS /
     >END

>END

>---
```

(a) `1ns`

```
   &ZPG_QDOT_PARAMETERS            T_wall = 288.0,
                               platelength = 0.60,
                                  xpoints = 100,
                                shockcase = 2,
                            RefTempMethod = 1,
                                  prandtl = 0.72,
                   Reynolds_analogy_factor = 1.1 /
```

(b) `1ns_zpg`

```
                          * * * CONE * * *

 Mach Num.    Re/x[1/m]   D[kg/m^3]    StatT[K] LAdWallT[K] TAdWallT[K]

     7.148   3.041E+07   1.259E-01        75.2       707.3       741.1


                         Local cf, delta_nu = nu_wall/u_tau and q_dot
                         --------------------------------------------

                                                  RefTempMethod
                                                 1. Eckert (1955)

           x =  0.600  Van Driest    Spalding   Lam Ref.T   Tur Ref.T

           T_wall [K]       288.0       288.0       288.0       288.0

                  F_c       3.558       3.558       4.262       4.360
                F_Rex       0.099       0.227       0.076       0.073
                Rex_i   1.810E+06   4.147E+06   1.391E+06   1.335E+06
               T* [K]         ---         ---       320.684     328.111

                   cf   1.096E-03   9.289E-04   2.288E-04   9.508E-04

          delta_nu [m]   9.596E-06   1.043E-05   2.100E-05   1.030E-05

          qdot [W/m^2]   4.451E+04   3.771E+04   9.697E+03   3.860E+04


                         Total heat transfer rate per unit plate width
                         ---------------------------------------------

           x =  0.600  Van Driest    Spalding   Lam Ref.T   Tur Ref.T

           Qdot [W/m]   2.960E+04   2.508E+04   6.592E+03   2.567E+04


                        Radiation and wall heat transfer rates: Case 0
                        ----------------------------------------------

                        User input: wall temperature [K] =  288.0

           x =  0.600  Van Driest    Spalding   Lam Ref.T   Tur Ref.T

          qr_dot [W/m]   0.000E+00   0.000E+00   0.000E+00   0.000E+00

          qs_dot [W/m]   4.451E+04   3.771E+04   9.697E+03   3.860E+04
```

(c) `zpgout.txt`

Figure B3: `zpg_qdot` file input-output for Chien (1974) case $T_w/T_0 = 0.35$. (a) `cmpexp` input. (b) `zpgqdot` input. (c) `zpgqdot` output.

In the CFD runs, 500 iterations were performed on each of three coarse grid levels, while the CFL number was increased linearly from 0.1 to 3.0 over each level. A multi-grid I cycle was used, and a higher-order solution was obtained on all grid levels. Iteration proceeded on the finest grid level until six orders of magnitude reduction in the residuals was achieved. The CFL number was increased linearly from 0.1 to 3.0 over the first 1500 iterations on the fine grid, and then was raised to 30.0 over a further 5000 iterations.

Figure B4 shows the sum of the density residuals from the CFD calculations of the Chien (1974) Mach 7.9 laminar and turbulent 5° semi-angle cone boundary layers. Among the laminar cases, a reduction of six orders of magnitude was only achieved for $T_w/T_0 = 0.35$. For the remaining two laminar cases with colder walls, the residuals tended to plateau somewhat above the required six orders of magnitude reduction level. The iterations were stopped at this point in both cases. The residuals for all the turbulent cases were reduced by the full six orders of magnitude. However, the residuals were reduced more slowly as the wall temperature was decreased. Finally, the choice of the k–ω or Menter-SST turbulence model had little influence on the evolution of the residuals for the case with $T_w/T_0 = 0.35$.

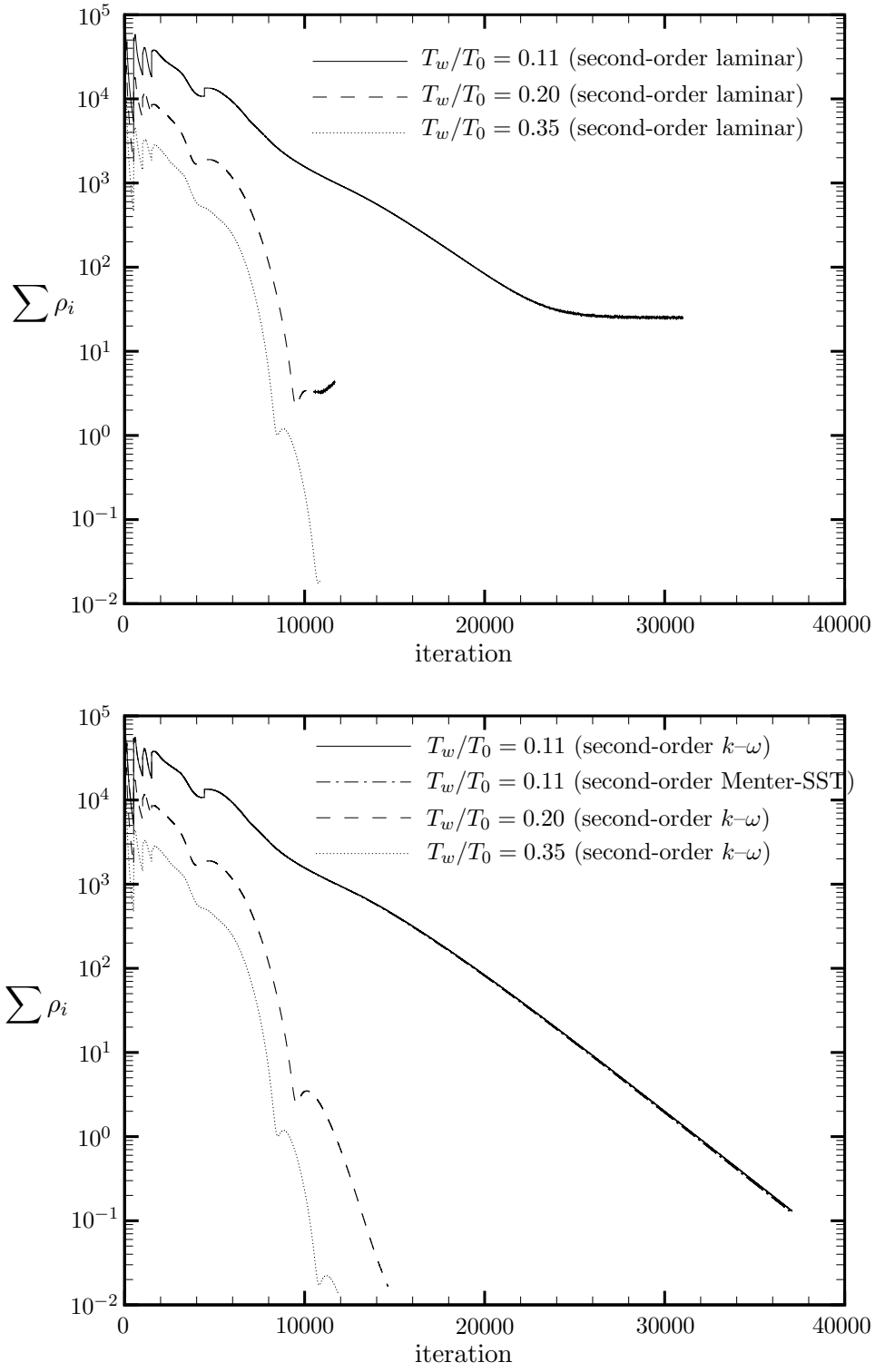

Figure B4: Sum of the density residuals from the CFD calculations of the Chien (1974) Mach 7.9 laminar and turbulent 5° semi-angle cone boundary layers shown in figures 10–12.

Appendix C Mach 8 flat plate, 10° wedge and cone at 35 km

Figures C1–C3 summarize the `zpg_qdot` input files `1ns` and `1ns_zpg` and output file `zpgout.txt` used to compute boundary layer properties at $x = 1.0\,\mathrm{m}$ from the leading edge of the Mach 8 flat plate and $x' = 1.0\,\mathrm{m}$ from the leading edge of the Mach 8 10° semi-angle wedge and cone cases with reference conditions listed in table 6. Table C1 summarizes the local viscous length scales at 1.0 m from the leading edge of the flat plate, wedge and cone obtained from the output file `zpgout.txt` shown in figures C1–C3. These length scales were used to determine the wall-normal and stream-wise CFD grid spacings using the rules described in Appendix A. Tables C2 and C3 summarize the details of the grids `fltplt_M8.dat`, `wedge10deg_M8.grd` and `cone10deg_M8.grd` used in the flat plate, wedge and cone calculations.

	flat plate	10° wedge	10° cone
laminar δ_ν (m)	6.4×10^{-5}	1.9×10^{-5}	1.9×10^{-5}
turbulent δ_ν (m)	3.5×10^{-6}	8.4×10^{-6}	1.1×10^{-5}

Table C1: Local viscous length scales computed with the Eckert (1955) reference temperature method at $x = 1.0\,\mathrm{m}$ from the leading edge of a Mach 8 flat plate and $x' = 1.0\,\mathrm{m}$ from the leading edge of a Mach 8 10° semi-angle wedge and cone at an altitude of 35 km.

$x_{\max}$ (m)	1.0
$y_{\max}$ (m)	0.1
$i_{\max}$	513
$j_{\max}$	97
$\Delta_n(i_{\min}, j_{\min})$ (m)	4.0×10^{-6}
$\Delta_n(i_{\max}, j_{\min})$ (m)	2.0×10^{-5}
$\Delta_n(i_{\text{min–max}}, j_{\max})$ (m)	7.0×10^{-3}
$\Delta_s(i_{\min}, j_{\text{min–max}})$ (m)	4.0×10^{-5}
$\Delta_s(i_{\max}, j_{\text{min–max}})$ (m)	1.3×10^{-2}

Table C2: Grid parameters used in constructing `fltplt_M8.grd`. Here Δ_n and Δ_s are the stream-wise and wall-normal grid spacings respectively.

$x'_{\max}$ (m)	1.00
$y'_{\max}$ (m)	0.15
$i_{\max}$	513
$j_{\max}$	97
$\Delta_n(i_{\min}, j_{\min})$ (m)	2.0×10^{-6}
$\Delta_n(i_{\max}, j_{\min})$ (m)	1.0×10^{-5}
$\Delta_n(i_{\text{min–max}}, j_{\max})$ (m)	1.3×10^{-2}
$\Delta_s(i_{\min}, j_{\text{min–max}})$ (m)	4.0×10^{-5}
$\Delta_s(i_{\max}, j_{\text{min–max}})$ (m)	1.3×10^{-2}

Table C3: Grid parameters used in constructing `wedge10deg_M8.grd` and `cone10deg_M8.grd`. Here x' and y' are coordinates parallel and normal to the surface of the wedge and cone in a stream-wise plane, and Δ_s and Δ_n are the associated stream-wise and wall-normal grid spacings.

```
>---

>TXT
      ***** Mach 8.00 flat plate inflow conditions *****
>END

>PRM
     &CMEX_PARAMETERS initial_pressure = 574.42,
                      initial_mach_number = 8.00,
                      default_initial_temperature = 236.47 /

     >SPC
        2
        N2  0.77
        O2  0.23
     >END

     >RUN
        2
        ISEN 1.0e0
        SHCK 1.300
     >END

     >RCT
        &REAC_PARAMETERS /
     >END

     >VOD
        &VODE_PARAMETERS /
     >END

>END

>---
```

(a) `1ns`

```
&ZPG_QDOT_PARAMETERS           T_wall = 300.0,
                           platelength = 1.0,
                               xpoints = 100,
                             shockcase = 0,
                          RefTempMethod = 1,
                               prandtl = 0.72,
                 Reynolds_analogy_factor = 1.1 /
```

(b) `1ns_zpg`

```
                    * * * FLAT PLATE * * *

Mach Num.   Re/x[1/m]   D[kg/m^3]    StatT[K] LAdWallT[K] TAdWallT[K]

    8.000   1.362E+06   8.426E-03       236.5      2439.0      2552.1


                        Local cf, delta_nu = nu_wall/u_tau and q_dot
                        --------------------------------------------

                                                    RefTempMethod
                                                   1. Eckert (1955)

          x =  1.000  Van Driest    Spalding   Lam Ref.T   Tur Ref.T

        T_wall [K]       300.0       300.0       300.0       300.0

               F_c       2.581       2.581       3.183       3.289
           F_Rex         0.321       1.712       0.131       0.123
           Rex_i     4.377E+05   2.331E+06   1.779E+05   1.679E+05
          T* [K]         ---         ---         752.785     777.672

              cf     1.707E-03   1.222E-03   4.945E-04   1.623E-03

      delta_nu [m]   3.427E-05   4.051E-05   6.368E-05   3.515E-05

      qdot [W/m^2]   5.222E+04   3.737E+04   1.618E+04   4.963E+04


                        Total heat transfer rate per unit plate width
                        ---------------------------------------------

          x =  1.000  Van Driest    Spalding   Lam Ref.T   Tur Ref.T

        Qdot [W/m]     6.533E+04   4.675E+04   2.866E+04   6.209E+04


                       Radiation and wall heat transfer rates: Case 0
                       ----------------------------------------------

                       User input: wall temperature [K] =  300.0

          x =  1.000  Van Driest    Spalding   Lam Ref.T   Tur Ref.T

      qr_dot [W/m]     0.000E+00   0.000E+00   0.000E+00   0.000E+00

      qs_dot [W/m]     5.222E+04   3.737E+04   1.618E+04   4.963E+04
```

(c) `zpgout.txt`

Figure C1: `zpg_qdot` file input-output for Mach 8 flat plate at 35 km. (a) `cmpexp` input. (b) `zpgqdot` input. (c) `zpgqdot` output.

```
>---

>TXT
      ***** Mach 8.00 10 degree wedge inflow conditions *****
>END

>PRM
     &CMEX_PARAMETERS initial_pressure = 574.42,
                      initial_mach_number = 8.00,
                      default_initial_temperature = 236.47 /

     >SPC
        2
        N2  0.77
        O2  0.23
     >END

     >RUN
        2
        ISEN 1.0e0
        SHCK 1.300
     >END

     >RCT
        &REAC_PARAMETERS /
     >END

     >VOD
        &VODE_PARAMETERS /
     >END

>END

>---
```

(a) `1ns`

```
&ZPG_QDOT_PARAMETERS           T_wall = 300.0,
                           platelength = 1.0,
                               xpoints = 100,
                             shockcase = 1,
                          RefTempMethod = 1,
                               prandtl = 0.72,
                 Reynolds_analogy_factor = 1.1 /
```

(b) `1ns_zpg`

```
                        * * * WEDGE * * *

Mach Num.   Re/x[1/m]   D[kg/m^3]    StatT[K] LAdWallT[K] TAdWallT[K]

    5.787   2.401E+06   2.425E-02       425.7      2461.6      2567.5


                        Local cf, delta_nu = nu_wall/u_tau and q_dot
                        --------------------------------------------

                                                  RefTempMethod
                                                 1. Eckert (1955)

          x =  1.000  Van Driest    Spalding   Lam Ref.T   Tur Ref.T

        T_wall [K]       300.0       300.0       300.0       300.0

               F_c       1.610       1.610       1.905       1.959
           F_Rex         0.810       4.166       0.324       0.308
           Rex_i     1.946E+06   1.000E+07   7.784E+05   7.399E+05
          T* [K]       ---         ---         810.740     834.047

              cf     2.031E-03   1.464E-03   3.952E-04   2.025E-03

      delta_nu [m]   8.408E-06   9.904E-06   1.906E-05   8.421E-06

      qdot [W/m^2]   1.743E+05   1.256E+05   3.643E+04   1.738E+05


                        Total heat transfer rate per unit plate width
                        ---------------------------------------------

          x =  1.000  Van Driest    Spalding   Lam Ref.T   Tur Ref.T

        Qdot [W/m]     2.179E+05   1.570E+05   6.439E+04   2.172E+05


                       Radiation and wall heat transfer rates: Case 0
                       ----------------------------------------------

                       User input: wall temperature [K] =  300.0

          x =  1.000  Van Driest    Spalding   Lam Ref.T   Tur Ref.T

      qr_dot [W/m]     0.000E+00   0.000E+00   0.000E+00   0.000E+00

      qs_dot [W/m]     1.743E+05   1.256E+05   3.643E+04   1.738E+05
```

(c) `zpgout.txt`

Figure C2: `zpg_qdot` file input-output for Mach 8 10° wedge at 35 km. (a) `cmpexp` input. (b) `zpgqdot` input. (c) `zpgqdot` output.

```
>---

>TXT
      ***** Mach 8.00 10 degree cone inflow conditions *****
>END

>PRM
     &CMEX_PARAMETERS initial_pressure = 574.42,
                      initial_mach_number = 8.00,
                      default_initial_temperature = 236.47 /

     >SPC
        2
        N2  0.77
        O2  0.23
     >END

     >RUN
        2
        ISEN 1.0e0
        SHCK 1.344
     >END

     >RCT
        &REAC_PARAMETERS /
     >END

     >VOD
        &VODE_PARAMETERS /
     >END

>END

>---
```

(a) `1ns`

```
&ZPG_QDOT_PARAMETERS           T_wall = 300.0,
                           platelength = 1.0,
                               xpoints = 100,
                             shockcase = 2,
                          RefTempMethod = 1,
                               prandtl = 0.72,
                 Reynolds_analogy_factor = 1.1 /
```

(b) `1ns_zpg`

```
                          * * * CONE * * *

Mach Num.   Re/x[1/m]   D[kg/m^3]    StatT[K] LAdWallT[K] TAdWallT[K]

    6.340   2.253E+06   1.989E-02       361.6      2453.9      2562.3


                        Local cf, delta_nu = nu_wall/u_tau and q_dot
                        --------------------------------------------

                                                    RefTempMethod
                                                   1. Eckert (1955)

          x =  1.000  Van Driest    Spalding   Lam Ref.T   Tur Ref.T

          T_wall [K]       300.0       300.0       300.0       300.0

                 F_c       1.830       1.830       2.188       2.254
               F_Rex       0.630       3.262       0.254       0.241
               Rex_i   1.420E+06   7.348E+06   5.731E+05   5.435E+05
              T* [K]         ---         ---     791.090     814.935

                  cf   2.237E-03   1.610E-03   6.943E-04   2.202E-03

        delta_nu [m]   1.048E-05   1.235E-05   1.881E-05   1.056E-05

        qdot [W/m^2]   1.589E+05   1.144E+05   5.290E+04   1.564E+05


                        Total heat transfer rate per unit plate width
                        ---------------------------------------------

          x =  1.000  Van Driest    Spalding   Lam Ref.T   Tur Ref.T

          Qdot [W/m]   1.689E+05   1.216E+05   5.398E+04   1.662E+05


                       Radiation and wall heat transfer rates: Case 0
                       ----------------------------------------------

                       User input: wall temperature [K] =  300.0

          x =  1.000  Van Driest    Spalding   Lam Ref.T   Tur Ref.T

        qr_dot [W/m]   0.000E+00   0.000E+00   0.000E+00   0.000E+00

        qs_dot [W/m]   1.589E+05   1.144E+05   5.290E+04   1.564E+05
```

(c) `zpgout.txt`

Figure C3: `zpg_qdot` file input-output for Mach 8 10° cone at 35 km. (a) `cmpexp` input. (b) `zpgqdot` input. (c) `zpgqdot` output.

In the CFD runs, 500 iterations were performed on each of three coarse grid levels, while the CFL number was increased linearly from 0.1 to 3.0 over each level. A multi-grid I cycle was used, and a higher-order solution was obtained on all grid levels. Iteration proceeded on the finest grid level until six orders of magnitude reduction in the residuals was achieved. The CFL number was increased linearly from 0.1 to 3.0 over the first 1500 iterations on the fine grid, and then was raised to 30.0 over a further 5000 iterations. Additionally, for the cone, an axisymmetric coordinate system with polar axis aligned with the local x axis was invoked.

Figure C4 shows the residuals and y^+ at the first grid point away from the wall for the laminar and turbulent Mach 8 flat plates at 35 km CFD runs using the Menter-SST turbulence model. The relative overall residual reduction of 6 orders of magnitude resulted in a reduction of about 5 orders of magnitude in the sum of the density residuals $\sum \rho_i$ for both the laminar and turbulent cases. Convergence was checked by restarting the calculations, reducing the residuals by a further 6 orders of magnitude, and then comparing the local heat transfer rate for the original and restarted results. For the Menter-SST and k–ω turbulence models, the two local heat transfer results differed by 0.10% and 0.16% respectively at $x = 0.1$m. Since the difference was small and the shape of the local heat transfer curves had not changed, convergence was assumed.

Two values of y^+ as a function of distance from the leading edge of the plate are also shown in figure C4. The solid line is the `plotprof2` output file `y+_fgp.dat`, while the dotted line is from the CFD output file `cfd.tec`. The factor-of-two discrepancy between `cfd.tec` and `y+_fgp.dat` was caused by the use of a cell-centered numerical scheme in the finite-volume CFD code, rather than a node-centred scheme used by `plotprof2`. The resulting y^+ from the CFD is then only one-half as large as the result computed by `plotprof2`. Nevertheless, the y^+ values are all well-below unity, apart from a few points immediately after the leading edge of the plate.

Figure C5 shows similar residuals and y^+ at the first grid point away from the wall for the turbulent Mach 8 10° wedge and cone at 35 km CFD runs using the Menter-SST turbulence model. Table C4 shows a summary of the shock angles used in `zpg_qdot` and estimated from the present CFD. It is evident that these angles are slightly smaller in the CFD calculations.

	10° wedge	10° cone
shock-wave angle from NACA (1953)	15.5°†	13.0°‡
shock-wave angle from present CFD	14.1°	12.2°

Table C4: Shock-wave angle for 10° semi-angle wedge and cone: †Chart 2, ‡Chart 5.

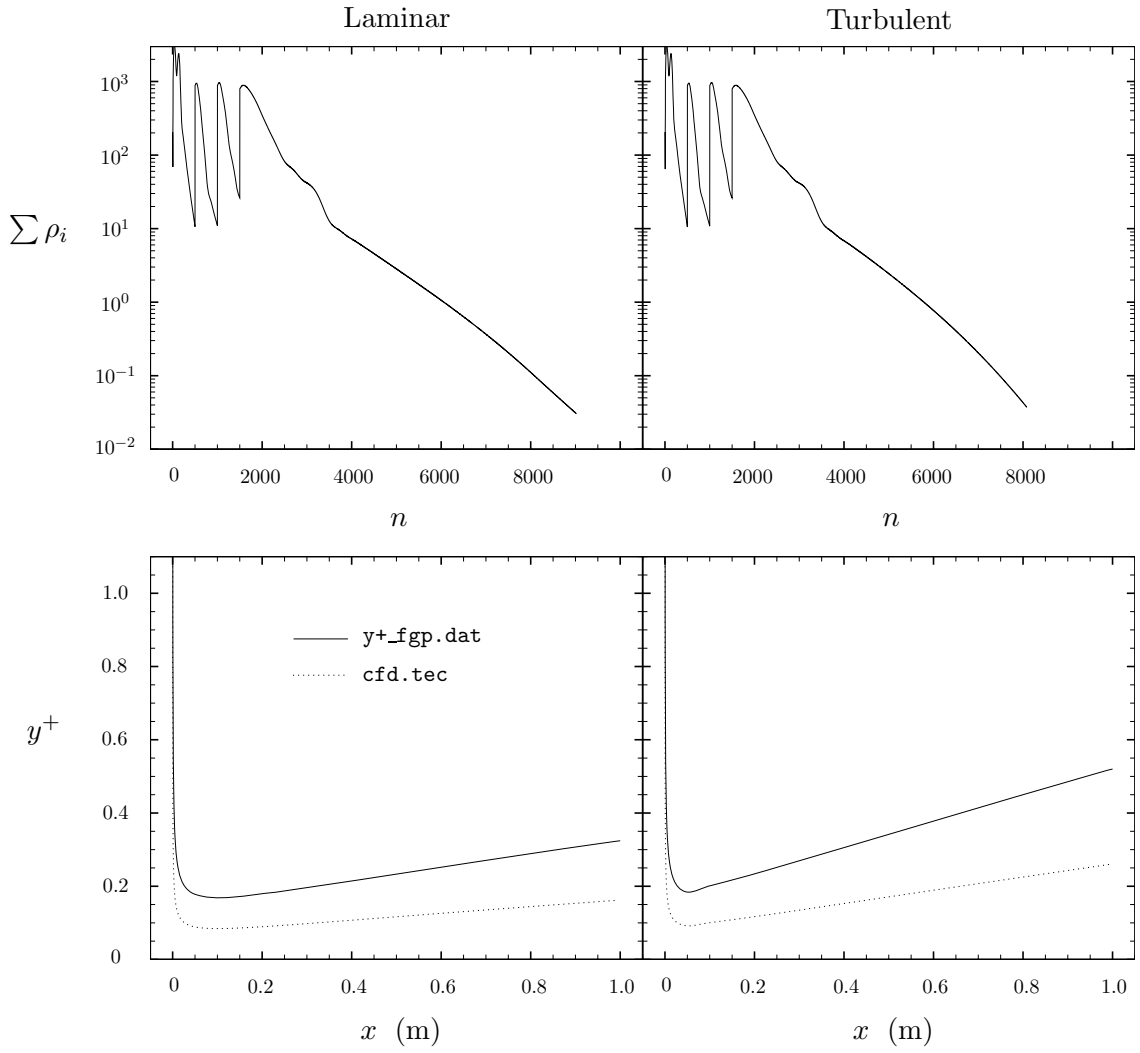

Figure C4: Residuals (upper panels) as a function of iteration number n and y^+ at the first grid point (lower panels) as a function of distance x from the leading edge for a compressible laminar (left) and turbulent (right) Mach 8 flat plate boundary layer at an altitude of 35 km. (Turbulent results computed with the Menter-SST model.)

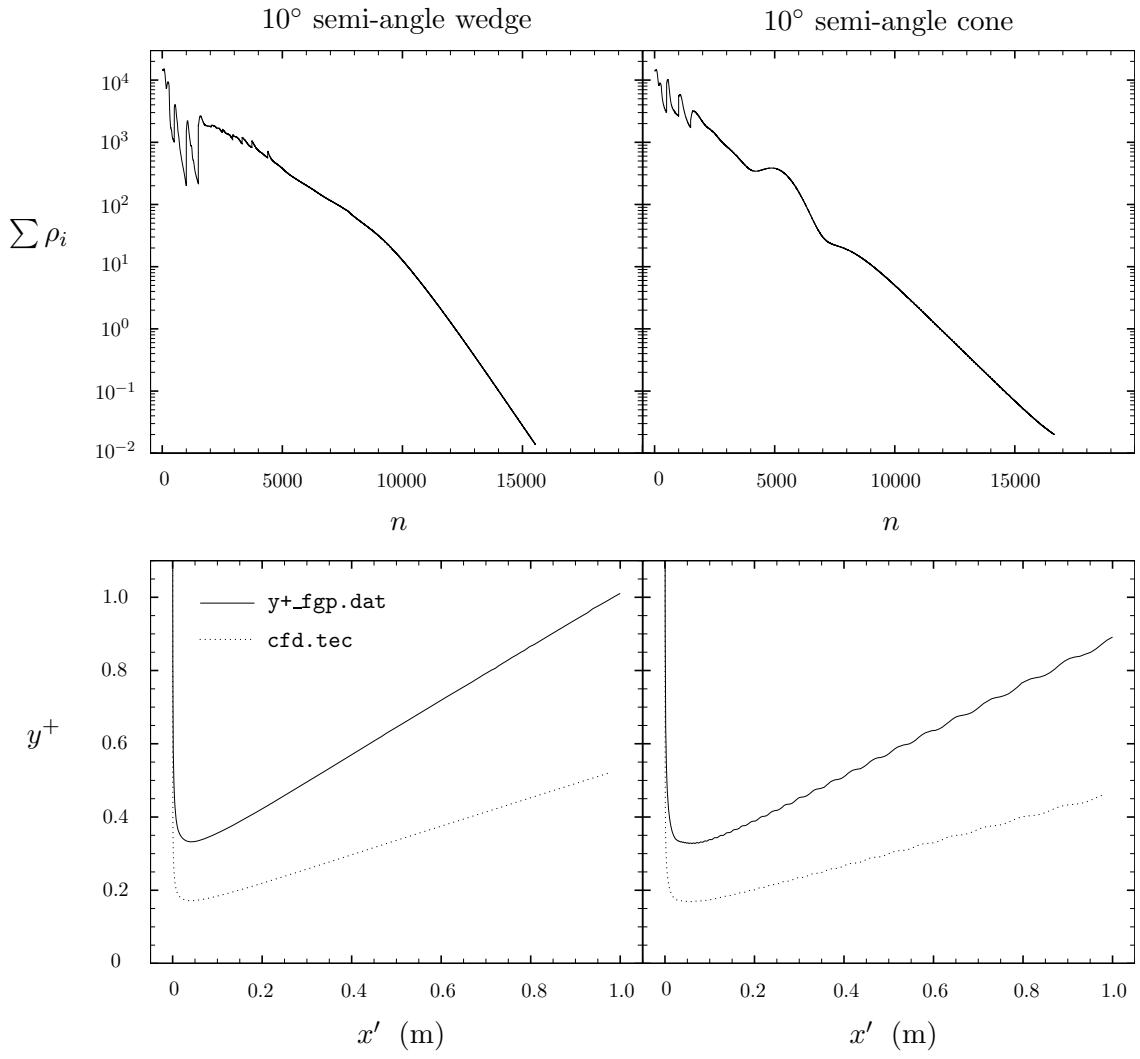

Figure C5: Residuals (upper panels) as a function of iteration number n and y^+ at the first grid point (lower panels) as a function of distance from the leading edge x' for a compressible turbulent Mach 8 boundary layer on a 10° semi-angle wedge (left) and cone (right) at an altitude of 35 km. The Menter-SST turbulence model was used in both cases.

Appendix D Mach 5 and 6 vitiated air flat plate boundary layers

Figures D2 and D3 summarize the `zpg_qdot` input files `1ns` and `1ns_zpg` and output file `zpgout.txt` used to compute boundary layer properties at $x = 1.0\,\mathrm{m}$ from the leading edge of the Mach 5 and 6 vitiated air flat plate boundary layer cases. Here vitiated air with the species mass fractions listed in table 7 was expanded isentropically to Mach 5 and 6 from the stagnation pressure, temperature and density of 3 MPa, 2204 K and $4.6697\,\mathrm{kg\,m^{-3}}$ respectively. These mass fractions and stagnation conditions were contained in a raw input file `cmex_rawin.txt` (generated by Dr. Nigel Smith, and not listed here) read directly by `cmpexp`. The pressure ratios used in the Mach 5 and 6 isentropic expansions were 1.15×10^{-3} and 3.50×10^{-4} respectively. The input files `1ns` listed in figures D2 and D3 run a normal shock and an isentropic compression following the isentropic expansions to Mach 5 and 6. Since `shockcase = 0` in the files `1ns_zpg`, the output from these processes is ignored, and the properties at the end of the first isentropic expansion only are used by `zpg_qdot`.

The turbulent viscous length scales computed with `zpg_qdot` at $x = 1\,\mathrm{m}$ from the leading edge of the Mach 5 and 6 vitiated flat plates were $\delta_\nu = 7.2\times10^{-6}\,\mathrm{m}$ and $2.0\times10^{-5}\,\mathrm{m}$ respectively. Since these were both larger than the viscous length scale determined earlier for the Mach 8 flat plate at 35 km ($3.5 \times 10^{-6}\,\mathrm{m}$), the grid used in that calculation was re-used in the present vitiated flat plate CFD. The Mach 8 flat plate multi-grid scheme and numerical method was also re-used. A detailed description of the Mach 8 flat plate grid and numerical method can be found in Appendix C. Figure D1 shows the residuals from the CFD calculations.

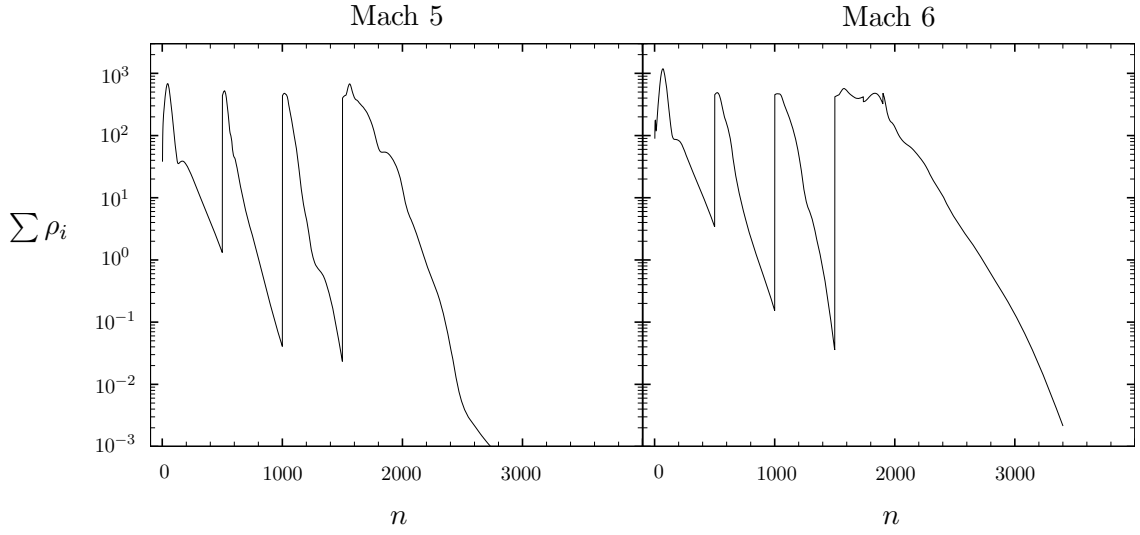

Figure D1: Residuals as a function of iteration number n for Mach 5 and 6 vitiated air turbulent flat plate boundary layers. The k–ω turbulence model was used in both cases.

```
>---

>TXT
     Expansion of vitiated air type ch4_air_o2_4159 through
     a nozzle to Mach 5.0 then through a normal shock
>END

>PRM
     &CMEX_PARAMETERS initial_pressure = 3.e6,
                      initial_mach_number = 0.0,
                      formation_temperature = 220. /

     >RUN
        3
        ISEN 1.15e-3
        SHCK 0.
        ISEN 1.2
     >END

     >RCT
        &REAC_PARAMETERS /
     >END

     >VOD
        &VODE_PARAMETERS /
     >END

>END

>---
```

(a) `1ns`

```
&ZPG_QDOT_PARAMETERS           T_wall = 300.,
                           platelength = 1.0,
                               xpoints = 100,
                             shockcase = 0,
                               prandtl = 0.72,
                Reynolds_analogy_factor = 1.1 /
```

(b) `1ns_zpg`

```
                    * * * FLAT PLATE * * *

Mach Num.   Re/x[1/m]   D[kg/m^3]    StatT[K] LAdWallT[K] TAdWallT[K]

    4.998   2.273E+06   2.574E-02       459.9      1960.6      2037.6


                    Local cf, delta_nu = nu_wall/u_tau and q_dot
                    --------------------------------------------

                                                  RefTempMethod
                                                 1. Eckert (1955)

          x =  1.000  Van Driest    Spalding   Lam Ref.T   Tur Ref.T

       T_wall [K]       300.0       300.0       300.0       300.0

              F_c       1.348       1.348       1.544       1.581
          F_Rex         1.061       4.393       0.455       0.436
          Rex_i     2.411E+06   9.985E+06   1.035E+06   9.913E+05
         T* [K]         ---         ---       710.092     727.027

             cf     2.323E-03   1.748E-03   4.227E-04   2.367E-03

     delta_nu [m]   7.291E-06   8.404E-06   1.709E-05   7.223E-06

     qdot [W/m^2]   1.551E+05   1.167E+05   3.037E+04   1.580E+05


                    Total heat transfer rate per unit plate width
                    ---------------------------------------------

          x =  1.000  Van Driest    Spalding   Lam Ref.T   Tur Ref.T

       Qdot [W/m]     1.939E+05   1.459E+05   5.366E+04   1.975E+05


                    Radiation and wall heat transfer rates: Case 0
                    ----------------------------------------------

                    User input: wall temperature [K] =  300.0

          x =  1.000  Van Driest    Spalding   Lam Ref.T   Tur Ref.T

     qr_dot [W/m]     0.000E+00   0.000E+00   0.000E+00   0.000E+00

     qs_dot [W/m]     1.551E+05   1.167E+05   3.037E+04   1.580E+05
```

(c) `zpgout.txt`

Figure D2: `zpg_qdot` file input-output for Mach 5 vitiated flat plate. (a) `cmpexp` input. (b) `zpgqdot` input. (c) `zpgqdot` output.

```
>---

>TXT
     Expansion of vitiated air type ch4_air_o2_4159 through
     a nozzle to Mach 6.0 then through a normal shock
>END

>PRM
     &CMEX_PARAMETERS initial_pressure = 3.e6,
                      initial_mach_number = 0.0,
                      formation_temperature = 220. /

     >RUN
        3
        ISEN 3.5e-4
        SHCK 0.
        ISEN 1.2
     >END

     >RCT
        &REAC_PARAMETERS /
     >END

     >VOD
        &VODE_PARAMETERS /
     >END

>END

>---
```

(a) `1ns`

```
&ZPG_QDOT_PARAMETERS           T_wall = 300.,
                           platelength = 1.0,
                               xpoints = 100,
                             shockcase = 0,
                               prandtl = 0.72,
                Reynolds_analogy_factor = 1.1 /
```

(b) `1ns_zpg`

```
                    * * * FLAT PLATE * * *

Mach Num.   Re/x[1/m]   D[kg/m^3]    StatT[K] LAdWallT[K] TAdWallT[K]

    5.999   1.273E+06   1.076E-02       334.8      1946.4      2028.0


                        Local cf, delta_nu = nu_wall/u_tau and q_dot
                        --------------------------------------------

                                                    RefTempMethod
                                                   1. Eckert (1955)

          x =  1.000  Van Driest    Spalding   Lam Ref.T   Tur Ref.T

        T_wall [K]       300.0       300.0       300.0       300.0

               F_c       1.720       1.720       2.007       2.061
           F_Rex         0.639       2.745       0.282       0.268
           Rex_i     8.133E+05   3.496E+06   3.586E+05   3.418E+05
          T* [K]         ---         ---         671.944     689.913

              cf     2.263E-03   1.691E-03   5.525E-04   2.247E-03

      delta_nu [m]   2.011E-05   2.327E-05   4.071E-05   2.019E-05

      qdot [W/m^2]   6.463E+04   4.828E+04   1.692E+04   6.417E+04


                        Total heat transfer rate per unit plate width
                        ---------------------------------------------

          x =  1.000  Van Driest    Spalding   Lam Ref.T   Tur Ref.T

        Qdot [W/m]     8.079E+04   6.035E+04   2.990E+04   8.021E+04


                       Radiation and wall heat transfer rates: Case 0
                       ----------------------------------------------

                       User input: wall temperature [K] =  300.0

          x =  1.000  Van Driest    Spalding   Lam Ref.T   Tur Ref.T

       qr_dot [W/m]    0.000E+00   0.000E+00   0.000E+00   0.000E+00

       qs_dot [W/m]    6.463E+04   4.828E+04   1.692E+04   6.417E+04
```

(c) `zpgout.txt`

Figure D3: `zpg_qdot` file input-output for Mach 6 vitiated flat plate. (a) `cmpexp` input. (b) `zpgqdot` input. (c) `zpgqdot` output.

DEFENCE SCIENCE AND TECHNOLOGY ORGANISATION DOCUMENT CONTROL DATA				1. CAVEAT/PRIVACY MARKING
2. TITLE Comparison of Engineering Correlations for Predicting Heat Transfer in Zero-pressure-gradient Compressible Boundary Layers with CFD and Experimental Data			3. SECURITY CLASSIFICATION Document (U) Title (U) Abstract (U)	
4. AUTHOR K. Higgins			5. CORPORATE AUTHOR Defence Science and Technology Organisation 506 Lorimer St, Fishermans Bend, Victoria 3207, Australia	
6a. DSTO NUMBER DSTO–TR–2159	6b. AR NUMBER 014-237		6c. TYPE OF REPORT Technical Report	7. DOCUMENT DATE August, 2008
8. FILE NUMBER 2007/1102911/1	9. TASK NUMBER 06/001	10. SPONSOR CDS	11. No OF PAGES 67	12. No OF REFS 17
13. URL OF ELECTRONIC VERSION http://www.dsto.defence.gov.au/corporate/reports/DSTO–TR–2159.pdf			14. RELEASE AUTHORITY Chief, Air Vehicles Division	
15. SECONDARY RELEASE STATEMENT OF THIS DOCUMENT *Approved For Public Release* OVERSEAS ENQUIRIES OUTSIDE STATED LIMITATIONS SHOULD BE REFERRED THROUGH DOCUMENT EXCHANGE, PO BOX 1500, EDINBURGH, SOUTH AUSTRALIA 5111				
16. DELIBERATE ANNOUNCEMENT No Limitations				
17. CITATION IN OTHER DOCUMENTS No Limitations				
18. DSTO RESEARCH LIBRARY THESAURUS Empirical methods, Heat transfer, Compressible flow, Boundary layers, Computational fluid dynamics				

19. ABSTRACT

The aim of this report is to investigate the details and performance of several engineering correlation methods used for predicting skin friction and heat transfer rates in high-speed flows. These are the van Driest, Eckert and Spalding & Chi correlations, which, in the form presented herein, can only be used for zero-pressure-gradient flows. This limits the scope of the report to flow past flat plates, and also wedges and cones with attached shock waves. The main result is a series of comparisons with experimental and CFD data of Stanton Numbers, heat transfer rates, skin friction coefficients and viscous length scales computed with the engineering correlations. Good agreement was observed among the laminar correlation, CFD and experimental data. Comparisons of turbulent correlation results with CFD and experimental data produced reasonable agreement in most cases, although the van Driest and Eckert correlations tended to over-estimate heat transfer rates on cold walls.